Review

Received: 6 May 2021 Accepted article published: 3 June 2021 Published online in Wiley Online Library: 19 June 2021

(wileyonlinelibrary.com) DOI 10.1002/pi.6264

Hydrogen bonding mediated self-assembled structures from block copolymer mixtures to mesoporous materials

Shiao-Wei Kuo*

Abstract

The self-assembled structures formed through hydrogen bonding interaction of block copolymers in polymeric materials are interesting materials because of their potential applications in biomedicine, nanopatterning and photonics, taking advantage of their responsive and tunable properties. In this review, we discuss the self-assembled nanostructures that can be obtained from hydrogen-bonded diblock copolymer/homopolymer (A-*b*-B/C) and diblock copolymer (A-*b*-B/C-*b*-D) mixtures in the bulk and how these block copolymer mixtures can then be used to synthesize mesoporous silica, phenolic and carbon materials.
© 2021 Society of Industrial Chemistry.

Keywords: self-assembly; hydrogen bonding; block copolymer; mesoporous materials; nanostructure

INTRODUCTION

Self-assembled supramolecular structures are relatively inexpensive and simple to prepare with large-scale nanopatterning from block copolymers, driven by a combination from repulsive interaction because of immiscibility and attractive interaction arising from the covalent linkage of their block segments. The well-defined self-assembled structures that have been observed from diblock copolymers in the bulk state have included alternative lamellae (LAM), hexagonally packed cylinder (HPC), body-centered cubic (BCC) and double-gyroid (DG) structures (Fig. 1(a)) and, in some cases, Frank–Kasper phase structures (e.g. A15 and σ phases). Furthermore, diblock copolymers can also self-assemble spontaneously in solution to form typical vesicle, rod (worm-like), sphere and other particular micellar structures (Fig. 1(b)).[1–10] The nature of these self-assembly behaviors in bulk or in solution depends primarily on the degree of polymerization (N), the interaction parameter (χ) and, most importantly, the volume fraction; the polydispersity, architecture, terminal functional units, common solvents, selective solvents, temperature and additives can also have influences.[11–19] Because the use of living polymerization to vary the volume fraction and the molecular weight of a block copolymer is generally synthetically complicated, the blending of block copolymers (e.g. A-*b*-B) with homopolymers or other block copolymers is a preferred approach for the preparation of various well-defined self-assembled nanostructures. In this review, we summarize the influence of hydrogen bonding strength on self-assembled nanostructures from block copolymer mixtures, and how this concept can be used to synthesize mesoporous silica, phenolic and carbon structures.

HYDROGEN BOND MEDIATED SELF-ASSEMBLY OF BLOCK COPOLYMERS

Hydrogen bonding results from dipole–dipole forces between strongly electronegative atoms (e.g. nitrogen (N) or oxygen (O) atoms) and hydrogen (H) atoms; the presence of hydrogen bonds in polymeric materials is of great interest because they can impart interesting surface, thermal, mechanical and optoelectronic properties.[15] Hydrogen bonding in block copolymers with low-molecular-weight compounds (e.g. long nonpolar alkyl units with polar head moieties such as phenolic and COOH groups) can result in comb-shaped materials displaying interesting hierarchical self-assembled structures; these systems have been studied widely for almost 30 years.[20–24] As mentioned above,[1–19] varying block segment volume fractions can have a dramatic effect on the different types of self-assembled structures that are formed, but this approach can be time-consuming, expensive and complicated when using living polymerization. Alternatively, blending diblock copolymers with homopolymers or diblock copolymers can provide various self-assembled structures because it imparts greater control over each volume fraction of the block segment. In the next sections, we discuss examples of the self-assembly behavior of diblock copolymer/homopolymer and diblock copolymer mixtures mediated through hydrogen bonding.

Diblock copolymer/homopolymer mixtures

Hashimoto and colleagues first reported the A-*b*-B diblock copolymers blending with A or B homopolymers, observing macrophase separation or order–order morphological transitions that strongly depended on the homopolymer's molecular weight.[25] Figure 2 displays three such cases: complete macrophase separation ($a > 1$) and 'dry-brush' ($a = 1$) and 'wet-brush' ($a < 1$)

* *Correspondence to: S-W Kuo, Department of Materials and Optoelectronic Science, Center of Crystal Research, National Sun Yat-Sen University, Kaohsiung, 80424, Taiwan. E-mail: kuosw@faculty.nsysu.edu.tw*

Department of Materials and Optoelectronic Science, Center of Crystal Research, National Sun Yat-Sen University, Kaohsiung, Taiwan

 © 2021 Society of Industrial Chemistry.

10970126, 2022, 4, Downloaded from https://onlinelibrary.wiley.com/doi/10.1002/pi.6264 by National Sun-Yat-Sen, Wiley Online Library on [15/11/2022]. See the Terms and Conditions (https://onlinelibrary.wiley.com/terms-and-conditions) on Wiley Online Library for rules of use; OA articles are governed by the applicable Creative Commons License

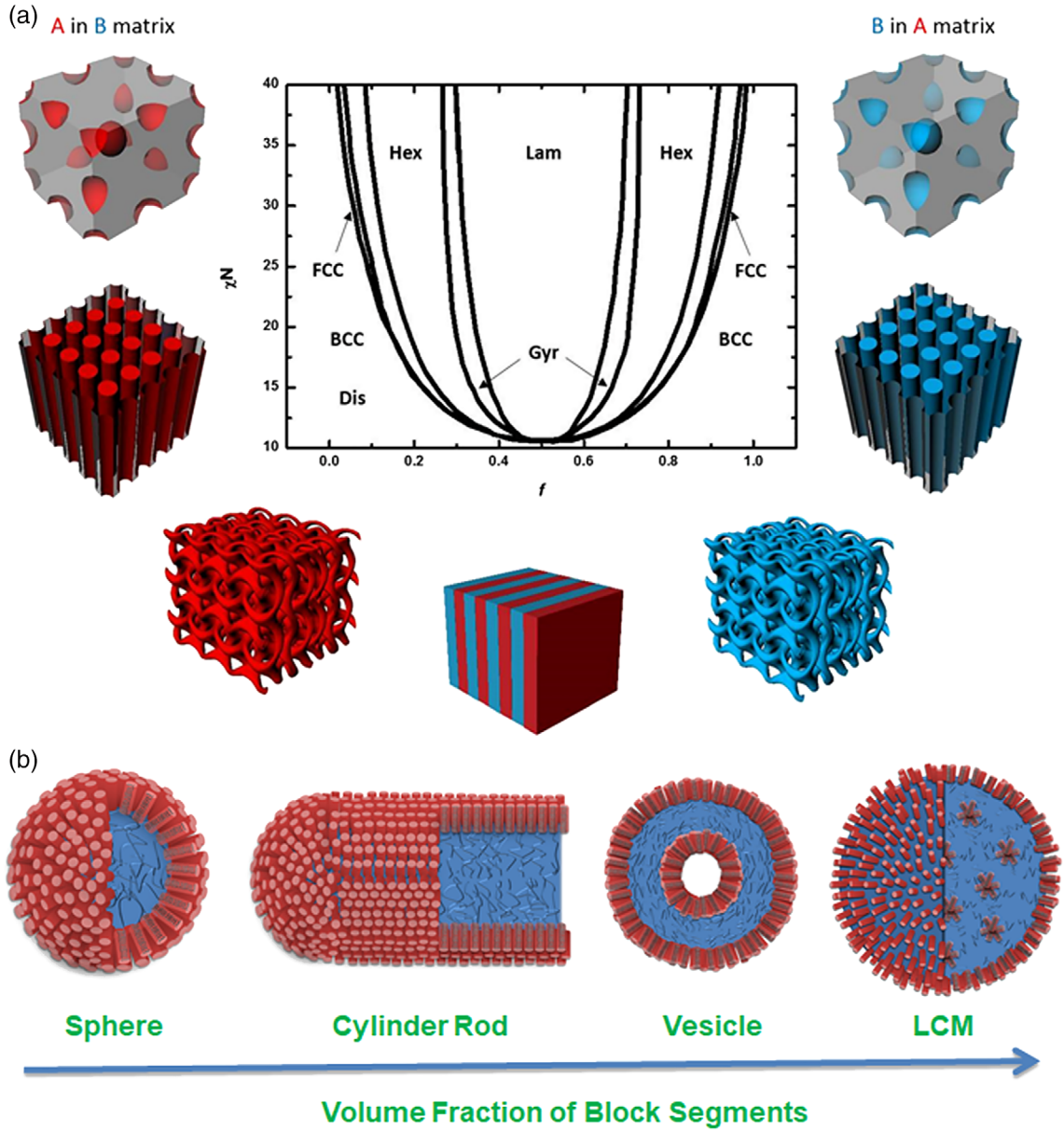

Figure 1. Typical self-assembled structures from diblock copolymer (a) in bulk and (b) in solution.[15]

behavior, where $a = M_{h\text{-}A}/M_{b\text{-}A}$ is the molecular weight ratio of the homopolymer to the A block segment.[15] In the wet-brush system, the homopolymer A is miscible with the A block, as expected, potentially resulting in a change in domain size or even in the type of self-assembled structure. In addition to A-*b*-B/A blends, A-*b*-B/C blends capable of hydrogen bonding have also undergone the order–order transition when the homopolymer C is capable of hydrogen bonding with either the A or the B segment. We have reported four different phenomena, either experimentally or theoretically, for such A-*b*-B/C blends during the last decade.[13,15,26]

Immiscible A/B diblock, miscible C/B but immiscible C/A binary pairs

Kwei and colleagues first proposed the possible phase behavior of A-*b*-B/C blends. Examples include the blending of the hydrogen-bond-accepting homopolymers (C) poly(4-vinylpyridine) (P4VP), poly(methyl methacrylate) (PMMA) and poly(ethylene oxide) (PEO) with poly(styrene-*b*-vinylphenol) (PS-*b*-PVPh) (A-*b*-B).[27] The PVPh block segment has phenolic OH units that could form intermolecular hydrogen bonding with these three homopolymers, although they are all immiscible with the PS block. Table 1 summarizes the inter-association equilibrium constants (K_A) for various hydrogen-bond-accepting homopolymers – including polyvinylpyrrolidone (PVP), P4VP, PEO, poly(caprolactone) (PCL), poly(vinyl acetate) (PVAc), PMMA, poly(vinyl phenyl ketone) (PVPK) and poly(lactide acid) (PLA) – blended with hydrogen-bond-donor PVPh segments (self-association equilibrium constant $K_B = 66.8$).[15,28] The Ikkala group reported the first self-assembled lamellae structure, obtained from phenolic resin (C) blended with poly(2-vinylpyridine)-*b*-polyisoprene (PI) (A-*b*-B), where the phenolic resin underwent hydrogen bonding and exhibited miscibility with the P2VP block but was immiscible with the PI segment.[29]

 © 2021 Society of Industrial Chemistry.

10970126, 2022, 4, Downloaded from https://onlinelibrary.wiley.com/doi/10.1002/pi.6264 by National Sun-Yat-Sen, Wiley Online Library on [15/11/2022]. See the Terms and Conditions (https://onlinelibrary.wiley.com/terms-and-conditions) on Wiley Online Library for rules of use; OA articles are governed by the applicable Creative Commons License

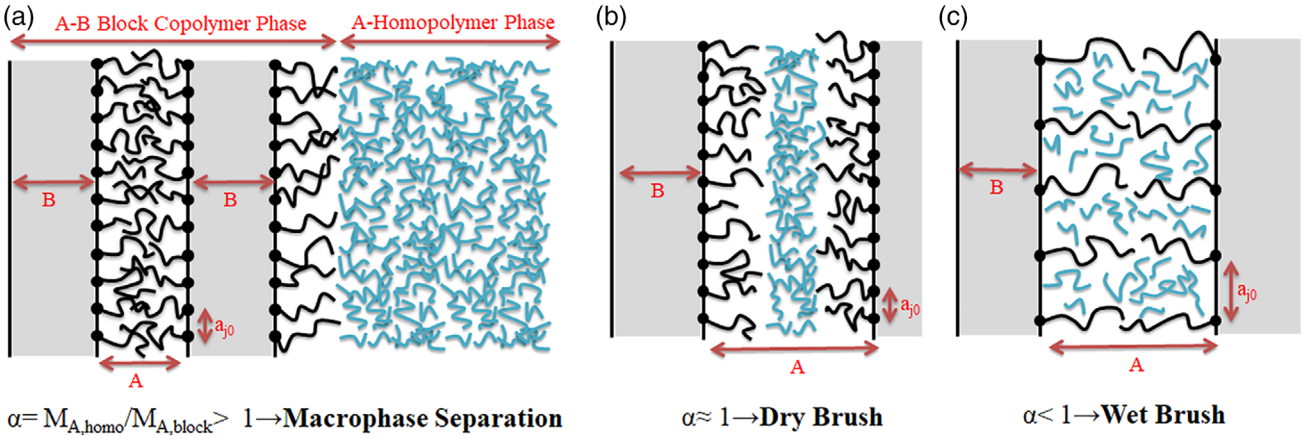

Figure 2. Phase behavior of diblock copolymer blending with homopolymers of various chain lengths (molecular weights): (a) macrophase separation, (b) dry brush and (c) wet brush.[15]

Table 1. Values of K_A for hydrogen bond acceptors interacting with PVPh ($K_B = 66.8$)[15]

H bond acceptor ($K_A > K_B$)	Molecular structure	K_A	H bond acceptor ($K_A < K_B$)	Molecular structure	K_A
PVP	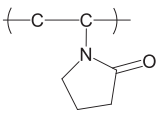	6000	PVAc	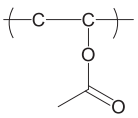	58
P4VP	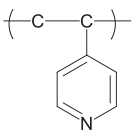	1200	PMMA	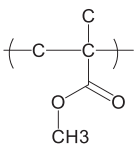	37
PEO	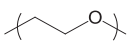	280	PVPK	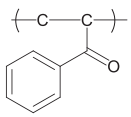	10
PCL	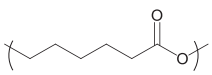	90	PLLA	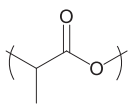	<10

Matsushita and colleagues systematically investigated the PVPh homopolymer (C) blending with PS-*b*-P2VP (A-*b*-B), where the PVPh/P2VP binary pair was miscible because of hydrogen bonding while PVPh was immiscible with the PS segment.[30] The molecular weight (degree of polymerization) of the PVPh homopolymer plays the key factor determining the nature of the self-assembled structure. For example, the use of PVPh of lower molecular weight (8 or 14 kDa) led to cylindrical structures, whereas PVPh of higher molecular weight (52 kDa) resulted in a lamellar structure when blended with PS-*b*-P2VP (34 kDa for the P2VP segment) at the same PS volume fraction ($f_{PS} = 0.48$), as displayed in Fig. 3.[31] When blending with shorter-chain-length PVPh, the distance between the junction points and the chain conformation was affected significantly relative to that observed with higher-molecular-weight PVPh. The high-molecular-weight PVPh did not undergo macrophase separation because the PVPh/P2VP domains featured strong hydrogen bonding, but only the entropy term of the Gibbs free energy was reported from that study.

As a result, we systematically investigated the enthalpy term (hydrogen bonding strength) of diblock copolymer/homopolymer mixtures capable of hydrogen bonding.[32,33] For example, we found that three hydrogen-bond-acceptor homopolymers (P4VP, P2VP, PMMA) of similar molecular weights provided similar entropy terms, but different enthalpy terms, when blending with a PS-*b*-PVPh and measuring their Gibbs free energies of mixing.[33] As revealed in Table 1, the values of K_A for PVPh/P4VP, PVPh/P2VP

© 2021 Society of Industrial Chemistry.

10970126, 2022, 4, Downloaded from https://onlinelibrary.wiley.com/doi/10.1002/pi.6264 by National Sun-Yat-Sen, Wiley Online Library on [15/11/2022]. See the Terms and Conditions (https://onlinelibrary.wiley.com/terms-and-conditions) on Wiley Online Library for rules of use; OA articles are governed by the applicable Creative Commons License

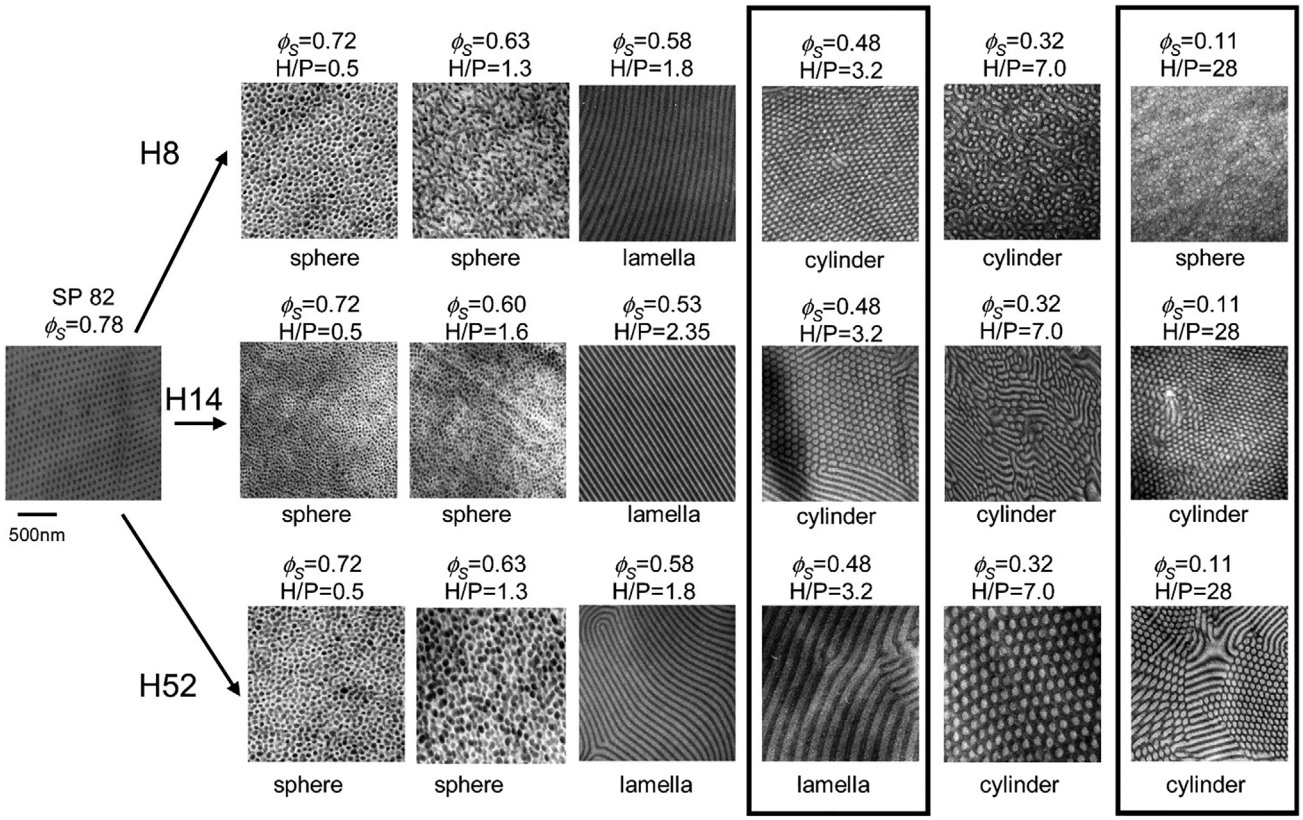

Figure 3. TEM images of PS-*b*-P2VP/PVPh mixtures incorporating PVPh homopolymers of various molecular weights and compositions.[31] (Reprinted with permission from American Chemical Society, 2009).

and PVPh/PMMA were 1200, 598 and 37.4, respectively; thus, the hydrogen bonding strength followed the order PVPh/P4VP > PVPh/P2VP > PVPh/PMMA. Figure 4(a) displays the self-assembled structures from the PS-*b*-PVPh/P4VP blends, which possess the strongest hydrogen bonding; a full order–order transition occurred from LAM to DG to HPC to BCC structures with the increase of P4VP concentration. Furthermore, Fig. 4(b) reveals that the self-assembled structures of PS-*b*-PVPh/P2VP blends also underwent an order–order transition from LAM to HPC to BCC structures upon increasing the P2VP concentration, but in this system we did not observe the DG structure. Therefore, blending with the strongly hydrogen bonding P4VP and P2VP homopolymer caused these A-*b*-B/C blends both to display wet-brush behavior. The blending of P4VP and P2VP with PS-*b*-PVPh resulted in BCC structures obtained at only 60 wt% P4VP and 70 wt% P2VP. In contrast, Fig. 4(c) reveals that the self-assembled structures of PS-*b*-PVPh/PMMA blends exhibited dry-brush behavior at lower PMMA concentrations with no morphological transitions, but higher PMMA concentrations led to macrophase separation.[33] The Shi group used the attractive interaction model featuring hydrogen bonding to theoretically predict the experimentally observed structures from A-*b*-B/C blends (Fig. 5(a)).[34] Based on the experimental and theoretical results, we confirmed that the strength of hydrogen bonding is an important factor in the behavior of such A-*b*-B/C blends. For example, when K_A/K_B was less than 1, dry-brush behavior was observed; when K_A/K_B was greater than 1, wet-brush behavior resulted and the systems displayed order–order transitions in the bulk state.[33] A-*b*-B/C blends have also been investigated recently with the A, B and C components being organic polymers or inorganic nanoparticles (e.g. gold, CdTe or polyhedral oligomeric silsesquioxane (POSS) nanoparticles), with strong hydrogen bonding interactions being present.[35–46]

Immiscible A/B diblock; C/A and C/B are both miscible binary pairs

The Kwei group proposed the first example of the system in which the A/B block pair was immiscible while the C/A and C/B binary pairs were both miscible; they were studying PS-*b*-PVPh/poly (vinyl methyl ether) (PVME) blends.[27] Because the PVME segment was miscible with both PVPh and PS segments, a PVME content of greater than 80 wt% in the ternary PS/PVPh/PVME blends resulted in miscible behavior, with the PVME acting as the common solvent for the PS and PVPh segments, stabilized through n–π and hydrogen bonding interactions, respectively. In contrast, when the PVME content was only 50 wt%, a single miscible phase was observed for the PS-*b*-PVPh/PVME blend, indicating that the covalent linkage in PS-*b*-PVPh resulted in a short-range attractive interaction that suppressed the macrophase separation.[27] Similar A-*b*-B/C blends where homopolymer C can undergo hydrogen bonding with both the A and B segments have been widely examined over the last decade.[47–59] In those studies, the value of ΔK was found to strongly influence the self-assembly behavior, e.g. when the B/C units (K_A) interact more strongly than the A/C units (K_C). As examples, consider the PCL-*b*-P2VP/PVPh or PCL-*b*-P4VP/PVPh blends that were first reported by the Guo group and by ourselves; here, the hydrogen-bond-donor PVPh homopolymer interacts intermolecularly with both the PCL and P2VP (or P4VP) segments, resulting in miscible behavior for these binary blend systems; nevertheless, the value of K_A for the interaction with the P2VP (or P4VP)

© 2021 Society of Industrial Chemistry.

10970126, 2022, 4, Downloaded from https://onlinelibrary.wiley.com/doi/10.1002/pi.6264 by National Sun-Yat-Sen, Wiley Online Library on [15/11/2022]. See the Terms and Conditions (https://onlinelibrary.wiley.com/terms-and-conditions) on Wiley Online Library for rules of use; OA articles are governed by the applicable Creative Commons License

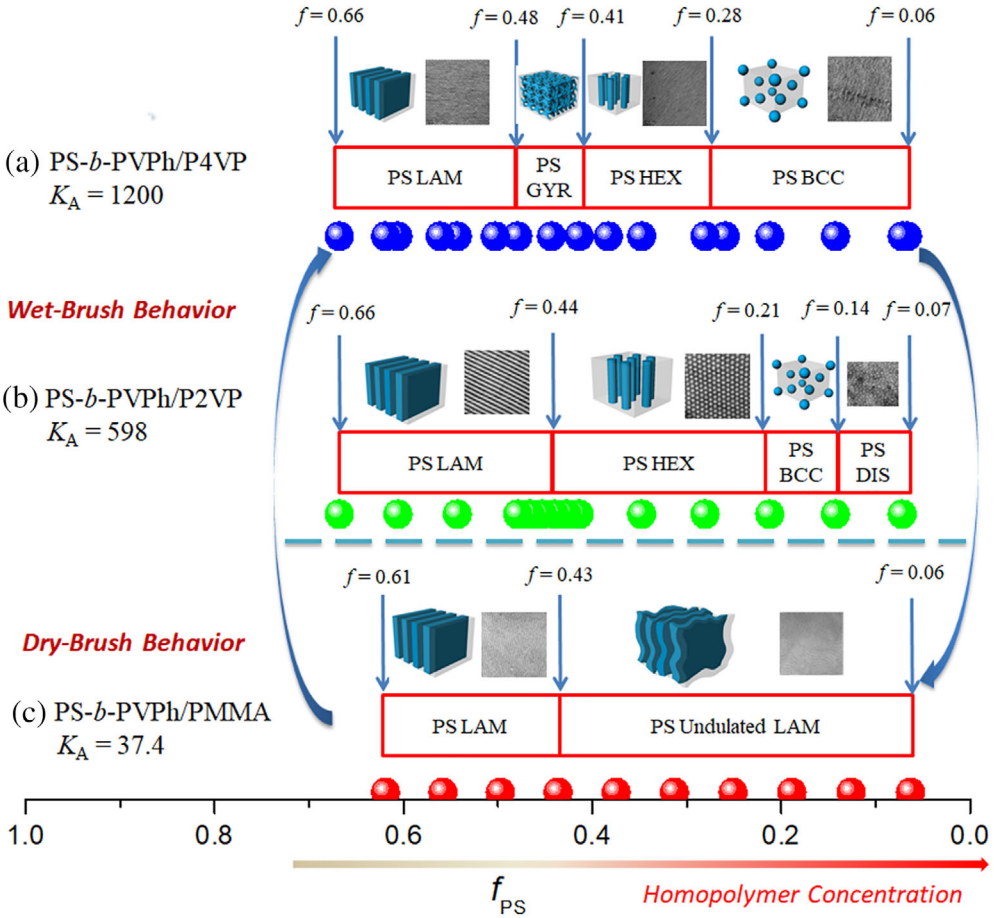

Figure 4. Self-assembled structures formed from PS-*b*-PVPh blended with various contents of (a) P4VP, (b) P2VP and (c) PMMA.[33]

block is higher than for the PCL segment (Table 1).[48,50] Various self-assembled structures were found as a result of this selective hydrogen bonding being dependent on the composition of PVPh. For example, Fig. 6 summarizes the glass transition temperatures (T_g) of PCL-*b*-P4VP/PVPh blends featuring miscible PVPh/P4VP pairs at various PVPh/PCL ratios.[50] At relatively low PVPh/PCL ratios (<0.7), the long-range-ordered sphere or cylinder structure was observed because the OH groups of the PVPh units preferred to interact with P4VP rather than PCL, suggesting a lower fraction of hydrogen-bonded PCL C=O groups ($f_b^{C=O}$ = 0–0.13). As a result, the long-range-order nanostructure was observed because the PCL segment would undergo phase separation from the miscible PVPh/P4VP phase. Increasing the PVPh/PCL ratio from 0.7 to 3 caused the OH groups of the PVPh units to interact also with PCL ($f_b^{C=O}$ = 0.15–0.45), thereby disrupting the PCL domains and causing the structures to transform into worm-like structures. A further increase in the PVPh/PCL ratio (>3.0) led to disordered structures because the larger content of OH groups resulted in a higher fraction of them being hydrogen bonded with the PCL segment ($f_b^{C=O}$ = 0.48–0.6).

Such A-*b*-B/C blends have also been prepared using PCL-*b*-P2VP/poly(acrylic acid) (PAA), P2VP-*b*-PMMA/phenoxy, PEO-*b*-PCL/PVPh, PCL-*b*-P2VP/phenoxy, PEO-*b*-PCL/phenolic, PEO-*b*-PCL/benzoxazine and P2VP-*b*-PMMA/PVPh blends.[51–59] Figure 7 outlines how competitive hydrogen bonding (ΔK effect) can determine the morphological transitions and self-assembled structures in these A-*b*-B/C blends.[56] In the first case, a disordered and completely miscible structure is found if the value of K_A is equal to that of K_C. In the second case, when the value of K_A is slightly higher than that of K_C, an ordered self-assembled structure (a BCC or HPC structure) is found at lower homopolymer C contents, becoming a miscible disordered structure at higher homopolymer C concentrations. In the final case, when the value of K_A is much higher than that of K_C, a full order–order transition occurs at lower homopolymer C contents, but a disordered structure exists at much higher homopolymer C concentrations.

Miscible A/B diblock; C/A and C/B are both miscible binary pairs

Miscible binary polymer blends featuring hydrogen bonding generally possess disordered and irregular structures and undergo uncontrollable assembly. Therefore, the preparation of regular ordered structures involving hydrogen bonding when the A/B, A/C and B/C binary pairs are individually miscible, but with different K_A values, has remained the great challenge. In ternary polymer blends, phase-separated closed-looped phase diagrams have been observed when all individual binary pairs are miscible, because of the ΔK effect.[60–63] Therefore, a third homopolymer C blended into the miscible A-*b*-B diblock copolymer may possess nanometer-scale self-assembled structures as a result of microphase separation. For example, PMMA-*b*-PVP/PVPh and PVPh-*b*-PMMA/PVP blends have all displayed such self-assembled structures.[64,65] Although PVPh is miscible with both PVP and PMMA through hydrogen bonding, the hydrogen bonding of the binary PVPh/PVP blend (K_A = 6000) is much stronger than that

© 2021 Society of Industrial Chemistry.

10970126, 2022, 4, Downloaded from https://onlinelibrary.wiley.com/doi/10.1002/pi.6264 by National Sun-Yat-Sen, Wiley Online Library on [15/11/2022]. See the Terms and Conditions (https://onlinelibrary.wiley.com/terms-and-conditions) on Wiley Online Library for rules of use; OA articles are governed by the applicable Creative Commons License

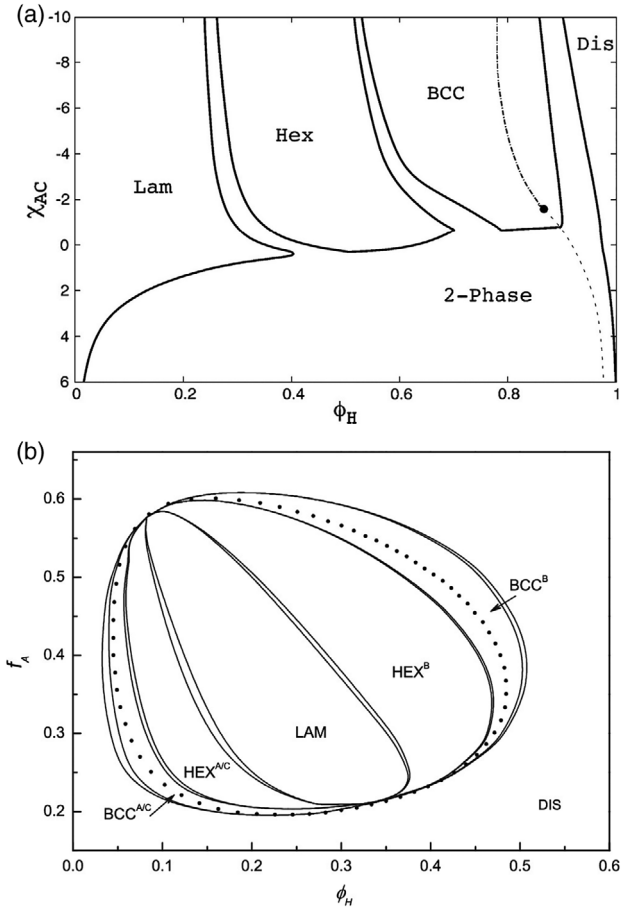

Figure 5. Predicted phase diagrams for A-*b*-B/C blends: (a) PS-*b*-PVPh/P2VP [34] and (b) PMMA-*b*-PVPh/PVP.[66] (Reprinted with permission from American Chemical Society, 2013, and AIP Publishing LLC, 2009).

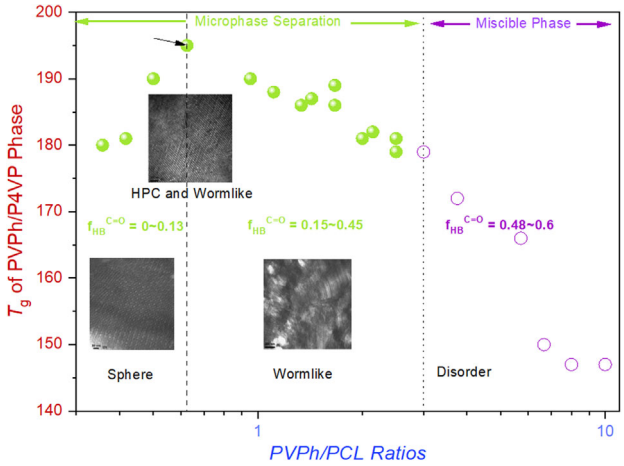

Figure 6. T_g values of the PVPh/P4VP domains in PCL-*b*-P4VP/PVPh mixtures at various PVPh/PCL ratios.[50]

of the binary PVPh/PMMA blend ($K_A = 37$), with the PVP and PMMA segments also being miscible. Microphase-separated closed-loop regions were found in such PVPh-*b*-PMMA/PVP blends, with the PMMA structures excluded from the miscible PVPh/PVP domains. DSC revealed that the miscible PVPh-*b*-PMMA became immiscible when the PVP content was 20–60 wt% (PMMA 57–26 wt%). At a lower PVP concentration (>56 wt% PMMA), the PMMA block could interact with the PVPh block through hydrogen bonding and form a miscible phase. Furthermore, the PMMA block was also miscible with the PVP at higher PVP contents (<27 wt% PMMA), stabilized through C=O···C=O dipole–dipole interactions. Thus, at these critical concentrations the systems could form unusual self-assembled structures, influenced by an intriguing balance of the PMMA concentration. For example, the LAM structure was observed when the PMMA content was 56 wt% (Fig. 8(a)), based on TEM, with the peak ratio of 1:2 based on small-angle X-ray scattering (SAXS) confirming the LAM structure. When the PMMA content was in the range 42–48 wt%, an HPC structure of PMMA micro-domains was formed (Figs 8(b), 8(c), based on TEM), with peak ratios of 1:√3:√4 confirming the HPC structure, based on SAXS analysis (Figs 8(f), 8(g)). Spherical self-assembled structures of PMMA micro-domains were observed when the PMMA content was 27 wt% (Fig. 8(d), based on TEM), with the SAXS pattern suggesting a mean diameter (*d*) of 8.1 nm (Fig. 8(h), dashed line).[65] This A-*b*-B/C blend has also been studied theoretically using self-consistent field theory.[66] A microphase-separation closed-loop phase diagram was observed because the A/B and A/C pairs possessed very different hydrogen bonding strengths (ΔK effect), even though all the binary pairs were individually miscible. The BCC, HPC and LAM structures were calculated to undergo an order–order morphological transition upon increasing the homopolymer concentrations (Fig. 5(b)); however, we did not find the inverse self-assembled nanostructures in an experimental setting upon increasing homopolymer contents.[66]

Miscible A/B diblock; miscible C/B and immiscible C/A binary pairs

The fourth case is when the A/B and B/C binary pairs are miscible but the A/C binary pair is immiscible, with hydrogen bonding of the B/C binary pair being significantly stronger than that of the A/B pair. The PCL-*b*-PVPh/PVP blend is an example of such a system that forms self-assembled structures. Here, the hydrogen bonding of the PVPh/PVP pair (B/C; $K_A = 6000$) is much stronger than that of the PVPh/PCL pair (A/B; $K_A = 90$), thereby inducing the self-assembled structure of a PCL micro-domain, as revealed in Fig. 9(A) through SAXS analyses.[67] The pure PCL-*b*-PVPh provides a broad scattering pattern, indicating a miscible disordered structure; scattering peaks gradually appear, however, upon increasing the content of PVP, because of the excluded PCL domains and the formation of highly ordered structures. For example, the LAM structure was characterized for PCL-*b*-PVPh/PVP = 50/50 mixture by SAXS peak ratios of 1:2:3; this structure was confirmed using TEM (Fig. 9(B)). The LAM structure transformed into an HPC structure upon increasing the content of PVP to 60–70 wt%, as evidenced by SAXS peak ratios of 1:√3:2 (Figs 9(A), curve (e)) and confirmed by TEM (Fig. 9(C)). Figure 9 (D) summarizes the self-assembly behavior.[67]

Diblock copolymer mixtures

A few types of self-assembled structures have only been observed for diblock copolymers, as mentioned above, with the LAM structure generally existing in a very narrow range of volume fraction when the two block segments are similar; thus, the symmetric LAM structure has usually been observed for block copolymers. Nevertheless, Kim and colleagues prepared interesting asymmetric LAM structures when blending highly asymmetric PS-*b*-PVPh diblock copolymers with highly asymmetric PS-*b*-P2VP or PS-*b*-P4VP diblock copolymers – namely, A-*b*-B/A-*b*-C blends where the B/C binary pairs are capable of hydrogen bonding (i.e. the

© 2021 Society of Industrial Chemistry.

10970126, 2022, 4, Downloaded from https://onlinelibrary.wiley.com/doi/10.1002/pi.6264 by National Sun-Yat-Sen, Wiley Online Library on [15/11/2022]. See the Terms and Conditions (https://onlinelibrary.wiley.com/terms-and-conditions) on Wiley Online Library for rules of use; OA articles are governed by the applicable Creative Commons License

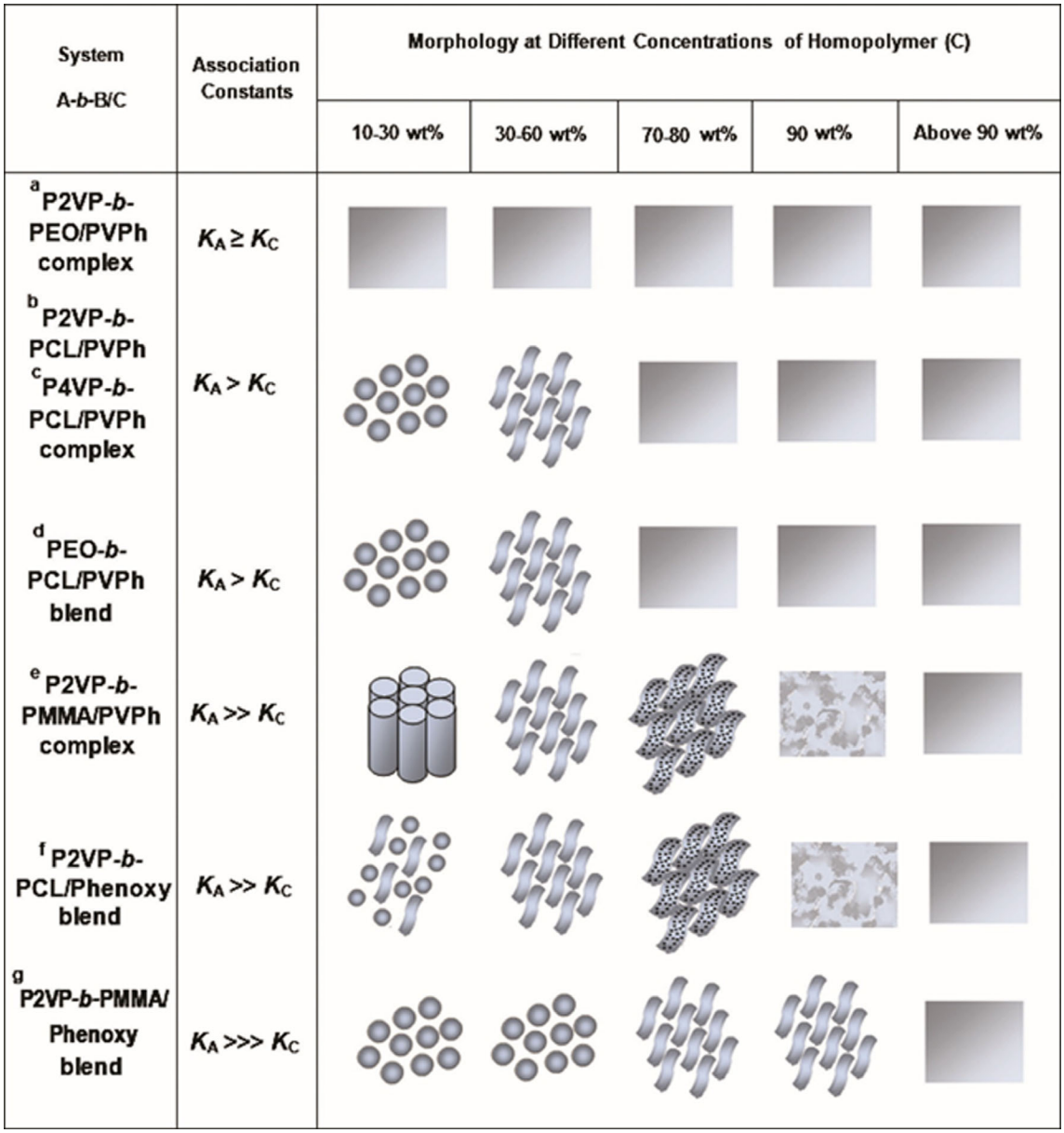

Figure 7. Proposed self-assembled structures of A-*b*-B/C blends in which the A/B diblock is immiscible but the C/A and C/B units are both miscible.[56] (Reprinted with permission from AIP Publishing LLC, 2009).

PVPh/P4VP and PVPh/P2VP binary pairs) while also featuring a highly asymmetric PS volume fraction ($f_{PS} = 0.8$).[68–72] Such structures are not usually observed for conventional diblock copolymers – the BCC spherical structures were observed in individual diblock copolymers, but they transformed into highly asymmetric LAM structures after blending (Fig. 10). A more highly asymmetric LAM structure formed when blending PS-*b*-P4VP, relative to that formed with PS-*b*-P2VP, since hydrogen bonding of P4VP is stronger than P2VP as expected.[68]

ABC triblock copolymers are also attractive since they can form self-assembled hierarchical structures different from those of diblock copolymers.[73–80] Nevertheless, using A-*b*-B/C-*b*-D blends and varying the hydrogen bonding strength is a relatively facile approach toward the preparation of such hierarchical structures while avoiding the generally complicated and difficult synthesis of ABC triblock copolymer.[81] We have found experimentally that three different phenomena occur in A-*b*-B/C-*b*-D mixtures featuring strong hydrogen bonds (Fig. 11).[82] Matsushita and colleagues first reported the blending of immiscible PS-*b*-PVPh (A-*b*-B) with immiscible P2VP-*b*-PI (C-*b*-D), where the PVPh/P2VP miscible binary pair featured strong hydrogen bonding but the PS/PI binary pair was immiscible.[83] Two different hierarchical structures were observed: (i) a LAM-within-LAM structure formed from PS_{50}-*b*-$PVPh_{50}$/$P2VP_{50}$-*b*-PI_{50} = 50/50 (Figs 12(a)–12(c)) and (ii) an isolated cylinder structure formed between the LAM layers from PS_{90}-*b*-$PVPh_{10}$/$P2VP_{10}$-*b*-PI_{90} = 50/50 (Figs 12(d)–12(f)) in which the miscible PVPh/P2VP domain featured an alternating LAM or isolated cylinder structure and the PI and PS blocks were arranged in alternate LAM structures.[83] We describe this A-*b*-B/C-*b*-D mixture as having a '2 + 2 = 3 phase' system, as shown in Fig. 11(a).

We have also investigated PS-*b*-PVPh blending with P4VP-*b*-PMMA or P4VP-*b*-PCL.[82,84] In these two blend systems, the PVPh

 © 2021 Society of Industrial Chemistry.

10970126, 2022, 4, Downloaded from https://onlinelibrary.wiley.com/doi/10.1002/pi.6264 by National Sun-Yat-Sen, Wiley Online Library on [15/11/2022]. See the Terms and Conditions (https://onlinelibrary.wiley.com/terms-and-conditions) on Wiley Online Library for rules of use; OA articles are governed by the applicable Creative Commons License

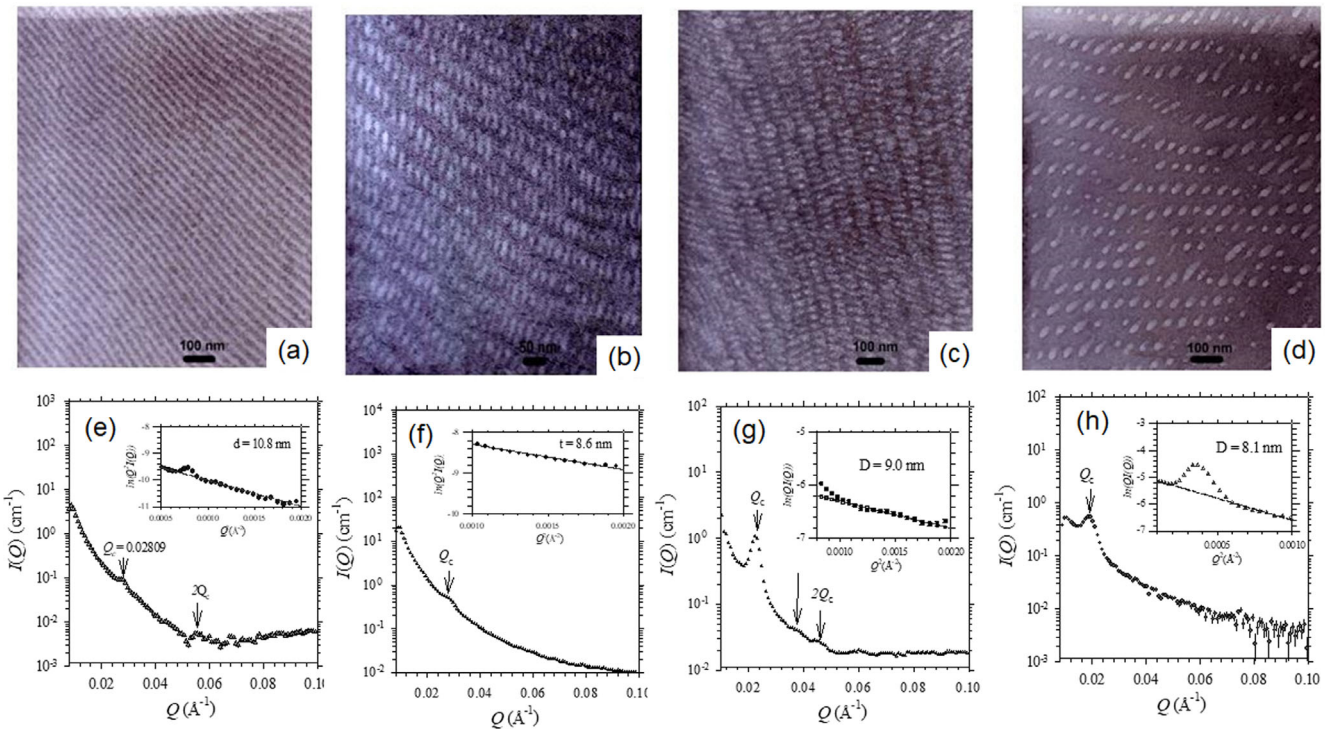

Figure 8. TEM and SAXS analyses of (a), (e) $PVPh_{30}$-*b*-$PMMA_{70}$/PVP = 80/20, (b), (f) $PVPh_{40}$-*b*-$PMMA_{60}$/PVP = 80/20, (c), (g) $PVPh_{30}$-*b*-$PMMA_{70}$/PVP = 60/40 and (d), (h) $PVPh_{55}$-*b*-$PMMA_{45}$/PVP = 60/40 blends.[65]

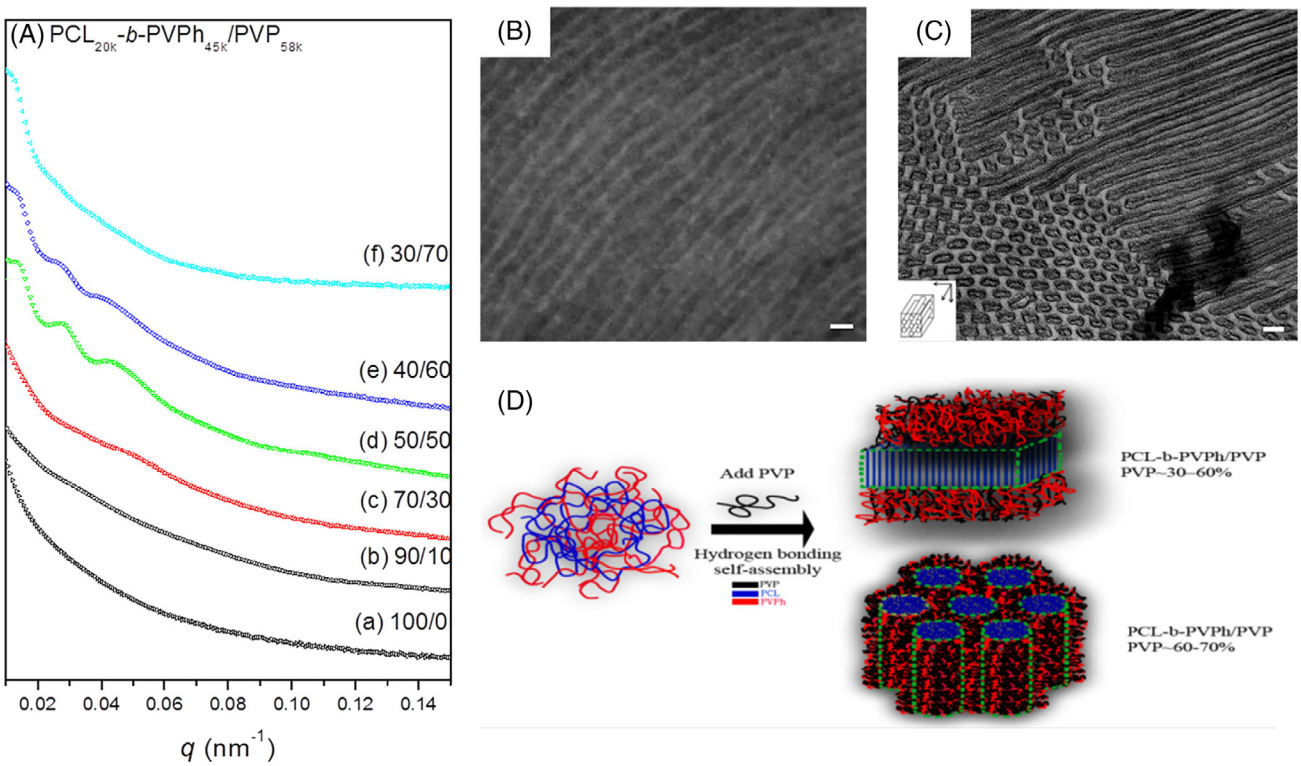

Figure 9. (A) SAXS patterns, (B), (C) TEM images and (D) possible self-assembled structures of PCL-*b*-PVPh/PVP blends.[67]

block can interact with both P4VP and PMMA/PCL segments, but the competitive hydrogen bonding can lead to various hierarchical structures – including core/shell HPC (Figs 13(a)–13(c)), HPC in LAM (Figs 13(d)–13(f)) and core/shell DG (Figs 13(g)–13(i)) structures – upon varying the blend compositions and volume fractions.[82]

We have found that a second system, the so-called '2 + 1 = 3 phase' system, formed when blending immiscible A-*b*-B with

© 2021 Society of Industrial Chemistry.

10970126, 2022, 4, Downloaded from https://onlinelibrary.wiley.com/doi/10.1002/pi.6264 by National Sun-Y at-Sen, Wiley Online Library on [15/11/2022]. See the Terms and Conditions (https://onlinelibrary.wiley.com/terms-and-conditions) on Wiley Online Library for rules of use; OA articles are governed by the applicable Creative Commons License

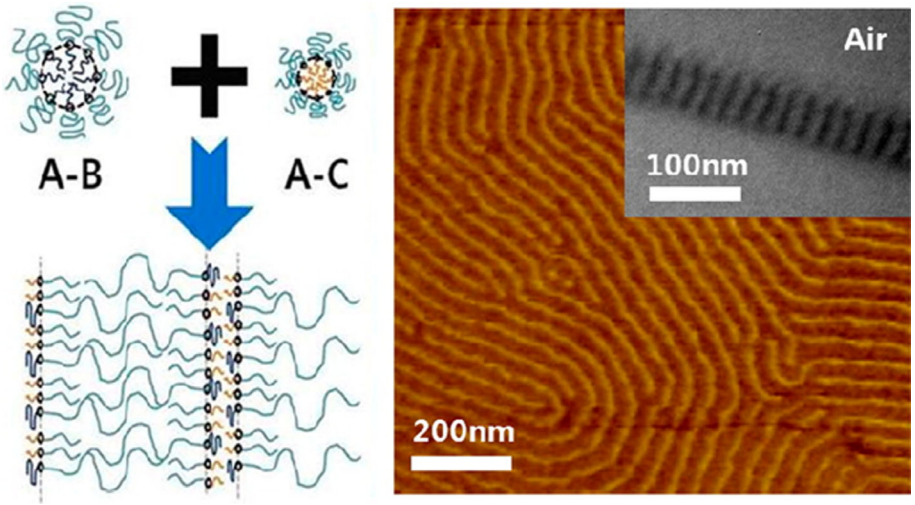

Figure 10. Schematic representation of asymmetric A-*b*-B/A-*b*-C blends and their asymmetric LAM structure based on TEM and AFM images.[68] (Reprinted with permission from American Chemical Society, 2012).

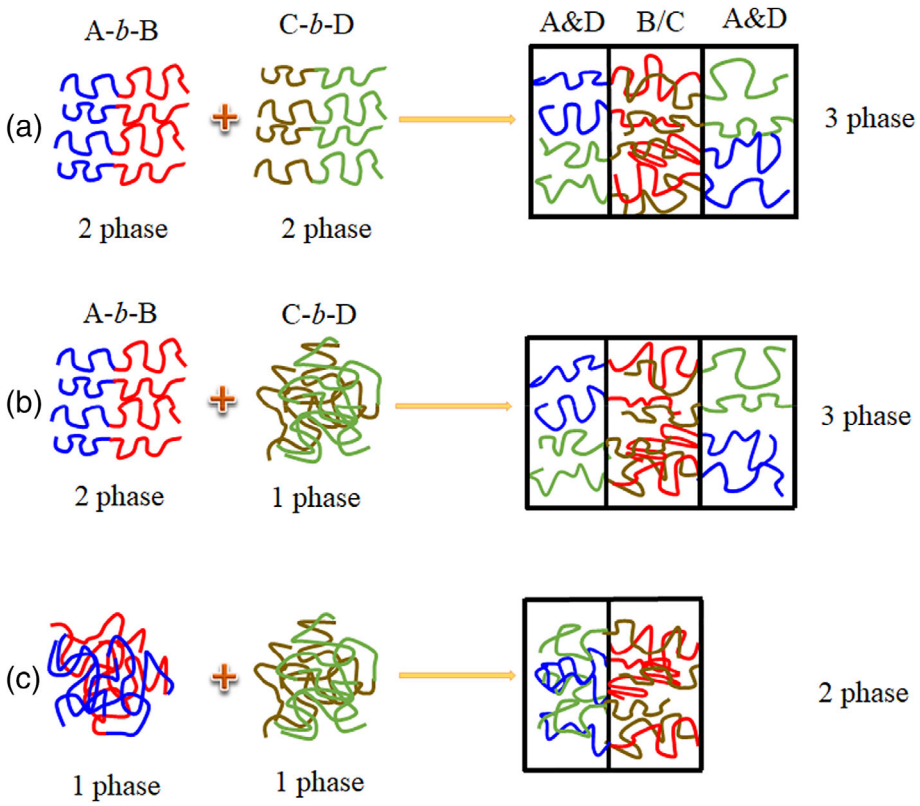

Figure 11. Cartoon representation of A-*b*-B/C-*b*-D mixtures stabilized through hydrogen bonding: (a) 2 + 2 = 3 phase, (b) 2 + 1 = 3 phase and (c) 1 + 1 = 2 phase.[82]

miscible C-*b*-D, as displayed in Fig. 11(b), e.g. PS-*b*-P4VP/PVPh-*b*-PMMA and PS-*b*-PVPh/P4VP-*b*-PEO mixtures.[85,86] These mixtures feature miscible PVPh/P4VP binary pairs and immiscible PS/PMMA or PS/PEO binary pairs, resulting in three-phase LAM (Figs 14(a), 14(b)) or core/shell (coaxial) HPC (Figs 14(c), 14(d)) structures.[85] We have also observed a third system formed from two miscible disordered PMMA-*b*-PVPh/P4VP-*b*-PEO blends, a so-called '1 + 1 = 2 phase' structure (Fig. 11(c)), featuring one miscible PMMA/PEO and another miscible PVPh/P4VP domain; two-phase behavior existed, providing both worm-like and LAM structures.[87]

More complicated block copolymer mixtures have been investigated from triblock copolymer/diblock copolymer mixtures. For example, Abetz and colleagues prepared PS-*b*-PB-*b*-poly(*tert*-butylmethacrylate) (PtBMA) (SBT, ABC) triblock copolymers by varying the degree of hydrolysis of the PtBMA segment (SBT) and blended them with P2VP-*b*-poly(cyclohexyl methacrylate) (PCHMA) and PS-*b*-P2VP (D-*b*-E).[88] Hierarchical self-assembled structures were

 © 2021 Society of Industrial Chemistry.

10970126, 2022, 4, Downloaded from https://onlinelibrary.wiley.com/doi/10.1002/pi.6264 by National Sun-Yat-Sen, Wiley Online Library on [15/11/2022]. See the Terms and Conditions (https://onlinelibrary.wiley.com/terms-and-conditions) on Wiley Online Library for rules of use; OA articles are governed by the applicable Creative Commons License

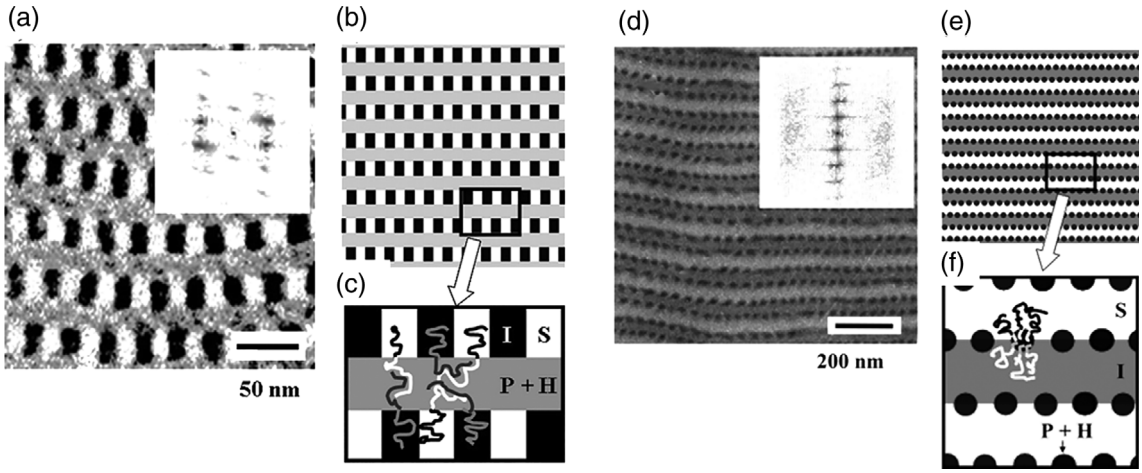

Figure 12. (a), (d) TEM images, (b), (e) schematic representation of the micro-domain arrangement and (c), (f) possible self-assembled structures of (a)–(c) PS_{50}-*b*-$PVPh_{50}$/$P4VP_{50}$-*b*-PI_{50} and (d)–(f) PS_{90}-*b*-$PVPh_{10}$/$P4VP_{10}$-*b*-PI_{90} = 50/50 blends.[83] (Reprinted with permission from American Chemical Society, 2005).

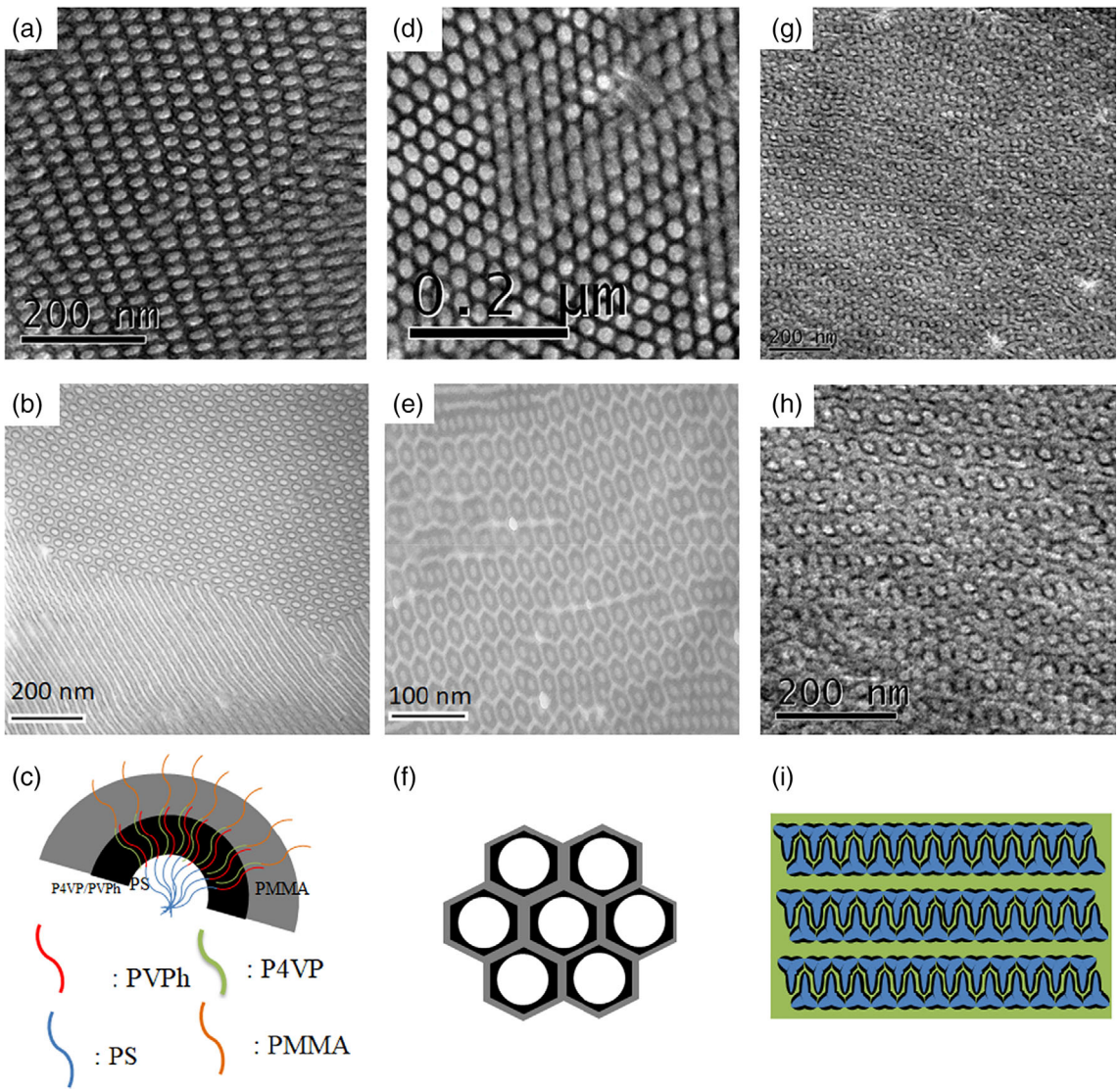

Figure 13. (a), (b) TEM images and (c) schematic representation of the possible core/shell HPC structure of PMMA-*b*-P4VP/PVPh-*b*-PS = 30/70. (d), (e) TEM images and (f) schematic representation of the possible close HPC within LAM structure of PMMA-*b*-P4VP/PVPh-*b*-PS = 20/80. (g), (h) TEM images and (i) schematic representation of the possible core/shell DG structure of PMMA-*b*-P4VP/PVPh-*b*-PS = 20/80. The PS domains appear white, the PVPh/P4VP domains appear dark and the PMMA domains appear gray in the TEM images.[82]

 © 2021 Society of Industrial Chemistry.

10970126, 2022, 4, Downloaded from https://onlinelibrary.wiley.com/doi/10.1002/pi.6264 by National Sun-Yat-Sen, Wiley Online Library on [15/11/2022]. See the Terms and Conditions (https://onlinelibrary.wiley.com/terms-and-conditions) on Wiley Online Library for rules of use; OA articles are governed by the applicable Creative Commons License

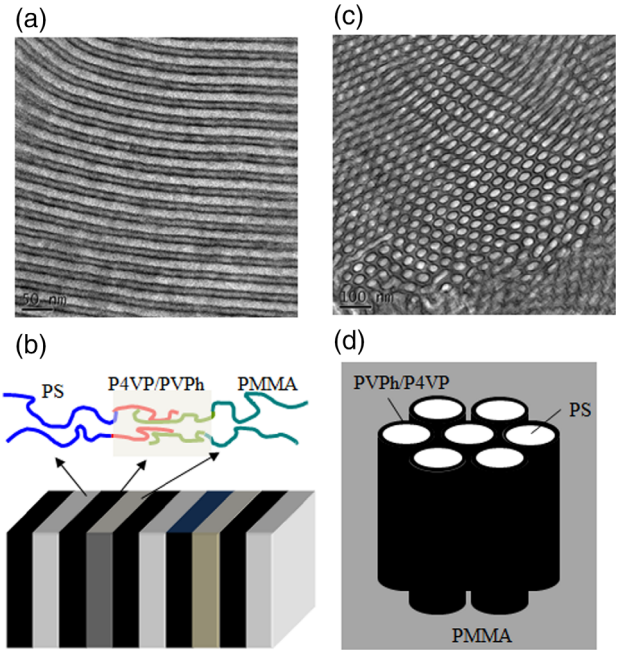

Figure 14. (a) TEM image and (b) schematic representation of the three-phase LAM structure of PS_{263}-*b*-$P4VP_{106}$/$PVPh_{137}$-*b*-$PMMA_{135}$ = 70/30. (c) TEM image and (d) schematic representation of the core/shell HPC structure of PS_{263}-*b*-$P4VP_{106}$/$PVPh_{137}$-*b*-$PMMA_{55}$ = 70/30.[85]

observed upon changing the hydrogen-bond-donor concentration of the SBT triblock copolymers. Matsushita and colleagues reported the blending of P2VP-*b*-PI-*b*-P2VP (ABA) with a PS-*b*-PVPh (C-*b*-D), where the PVPh/P2VP miscible binary pair featured strong hydrogen bonding[89] but the PS/PI binary pair was immiscible, similar to their previous study.[83] More complicated hierarchical structures were observed for the PS_{90}-*b*-$PVPh_{10}$/PI_{90}-*b*-$P4VP_{10}$-*b*-PI_{90} = 1/1 blend, forming a ($3^3.4^2$) Archimedean tiling pattern (Figs 15(a), 15(b)), and the PS_{90}-*b*-$PVPh_{10}$/PI_{90}-*b*-$P4VP_{10}$-*b*-PI_{90} = 2/1 blend, forming a (3.4.6.4) Archimedean tiling pattern (Figs 15(c), 15(d)).[89] They also studied the blending of the star PI-*b*-PS-*b*-P2VP (ABC) with a PVPh-*b*-PMMA (D-*b*-E), where PVPh/P2VP formed a miscible binary pair while the PI, PS and PMMA segments were individually immiscible; this system displayed a [4.8.8] Archimedean tiling (Fig. 16).[90] There are 11 Archimedean tiling patterns and we suspect that further explorations of diblock copolymer mixtures will reveal other examples of these hierarchical structures. In addition, diblock copolymer/homopolymer mixtures and diblock copolymer mixtures featuring hydrogen bonding of various strengths have also been found, over the last two decades, to self-assemble spontaneously into various interesting micellar structures.[91–105]

USING HYDROGEN-BONDED BLOCK COPOLYMER MIXTURES TO PREPARE MESOPOROUS MATERIALS

Mesoporous silica materials

Based on the IUPAC definition, mesoporous materials have pore sizes between 2 and 50 nm; when prepared by using block copolymers as templates, they have generally been formed with highly ordered structures featuring high surface area or high pore volume. As a result, the design of mesoporous silica and phenolic/

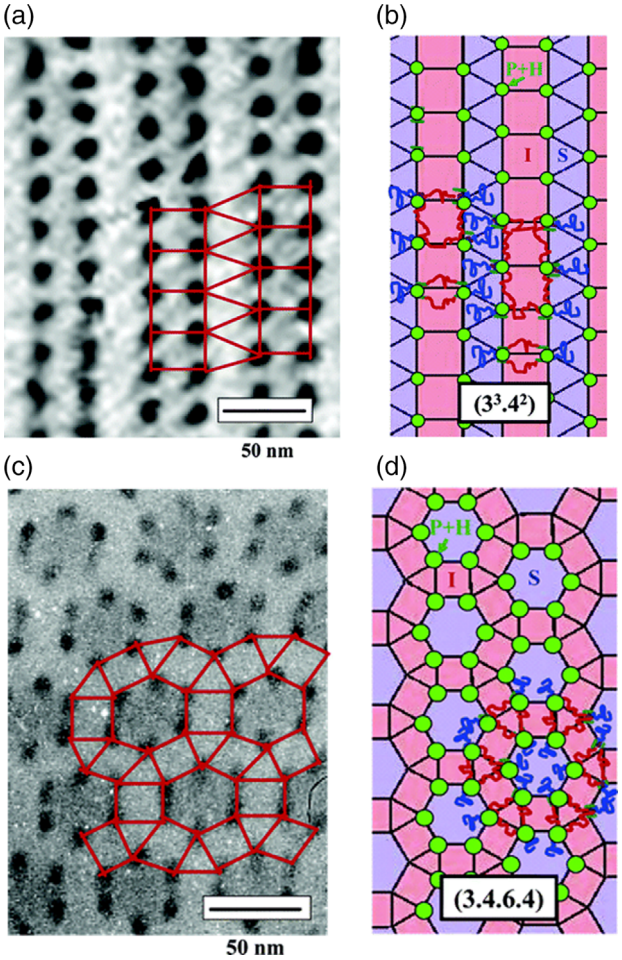

Figure 15. (a) TEM image and (b) schematic representation of the ($3^3.4^2$) Archimedean tiling pattern of the PS_{90}-*b*-$PVPh_{10}$/PI_{90}-*b*-$P4VP_{10}$-*b*-PI_{90} = 1/1 blend. (c) TEM image and (d) schematic representation of the (3.4.6.4) Archimedean tiling pattern of the PS_{90}-*b*-$PVPh_{10}$/PI_{90}-*b*-$P4VP_{10}$-*b*-PI_{90} = 2/1 blend.[89] (Reprinted with permission from American Chemical Society, 2006).

carbon materials is similar to that of diblock copolymer/homopolymer mixtures mediated by hydrogen bonds. Several factors can affect the synthesis of highly ordered mesoporous silicas, including (i) the nature of the hydrogen bonding between the silica precursor (tetraethyl orthosilicate (TEOS)) and the template, (ii) the self-assembly behavior of the template in response to the solvent, and (iii) the sol–gel process of TEOS (Fig. 17).[15]

Mesoporous silicas templated by block copolymers

The first example of mesoporous silicas templated by block copolymers involved the use of water-soluble PPO-*b*-PEO-*b*-PPO (ABA) (e.g. P123 and F127) and precipitation-based methods.[106–110] Nevertheless, most diblock copolymers are water-insoluble (e.g. PE-*b*-PEO, PEO-*b*-PCL, PEO-*b*-PS, PEO-*b*-PLA and PEO-*b*-PMMA) with long hydrophobic block segments; in this case, the evaporation-induced self-assembly (EISA) method can be used for the synthesis of large mesoporous silicas.[111–119] For example, we have used PEO-*b*-PCL as the template for the preparation of mesoporous silicas (Fig. 18).[115,116] Upon increasing the length of the PCL chain, the mesoporous silicas transformed from BCC to HPC structures, with the pore size increasing upon increasing the TEOS/PEO-*b*-PCL ratio.[116] In addition, we found that the

© 2021 Society of Industrial Chemistry.

10970126, 2022, 4, Downloaded from https://onlinelibrary.wiley.com/doi/10.1002/pi.6264 by National Sun-Yat-Sen, Wiley Online Library on [15/11/2022]. See the Terms and Conditions (https://onlinelibrary.wiley.com/terms-and-conditions) on Wiley Online Library for rules of use; OA articles are governed by the applicable Creative Commons License

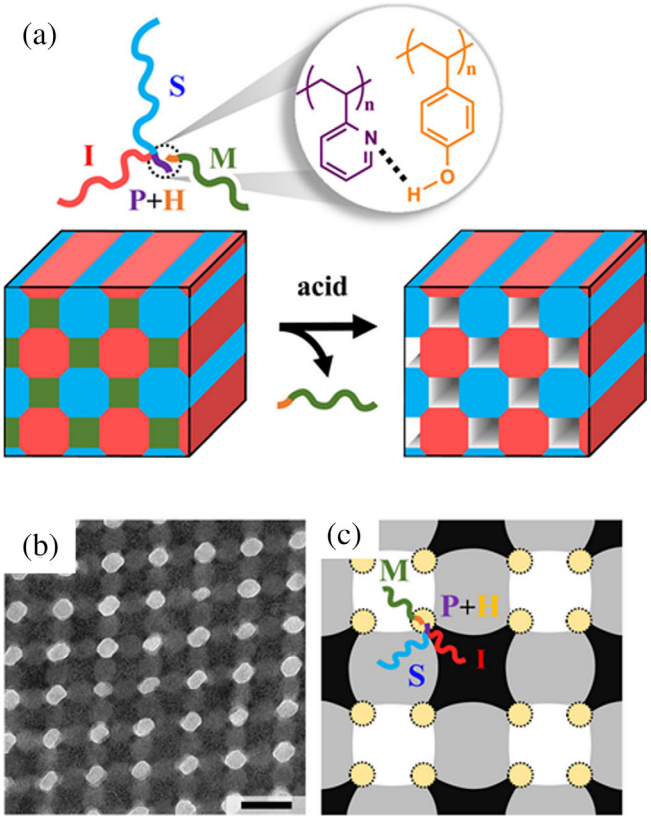

Figure 16. (a) Schematic representation of the star PI-*b*-PS-*b*-P2VP (ABC) triblock copolymer blended with PVPh-*b*-PMMA (D-*b*-E) and stabilized through hydrogen bonding interactions. (b) TEM image (scale bar 50 nm) of ISP/HM-0.30. (c) Schematic representation of the chain conformation and domain orientation, based on the TEM image; yellow, white, gray and black regions correspond to the PVPh/P2VP domain and PMMA, PS and PI phases, respectively.[90] (Reprinted with permission from American Chemical Society, 2017).

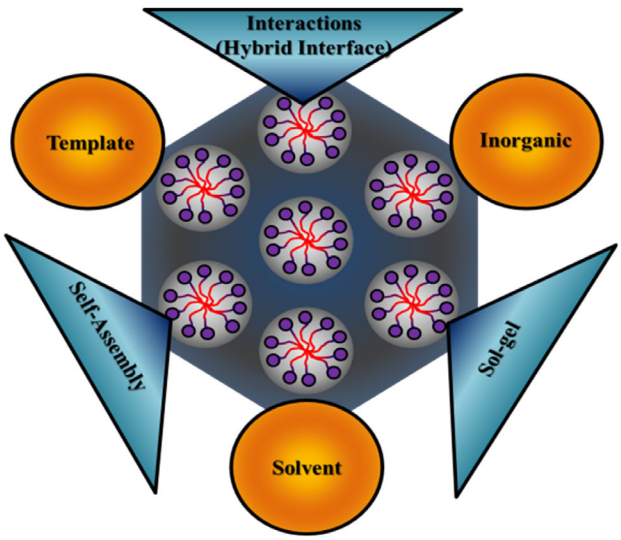

Figure 17. Main factors influencing the design of highly ordered mesoporous silicas.

solvent was another key factor affecting the synthesis of these mesoporous silicas. Improving the solubility or miscibility between the solvent (acetone, in this case) and the PEO-*b*-PCL diblock copolymer led to more highly ordered mesoporous silicas compared with those formed using tetrahydrofuran or CH_2Cl_2 as the solvent.[117]

Mesoporous silicas templated by block copolymer/homopolymer blends

As discussed above, blending A-*b*-B with homopolymers can be a facile approach for preparing different self-assembled structures; indeed, mesoporous silicas can also be prepared by using A-*b*-B/B mixtures as templates. For example, we reported mesoporous silicas templated by PEO-*b*-PCL/PEO and PEO-*b*-PCL/PCL blends.[116] When blended with the short-chain-length homopolymer PCL_{20}, the pore size was increased upon increasing PCL_{20} homopolymer concentrations due to the wet-brush behavior; the system displayed dry-brush behavior, however, when the blend contained the high-molecular-weight homopolymer PCL_{408}. Furthermore, an order–order mesophase transition occurred when blending with low-molecular-weight star PEO, because of improved miscibility within the silicas.[116]

Watkins and colleagues proposed mesoporous silicas templated by F127/PAA and F127/PVPh blends.[120] Compared with the use of F127 alone as the template, stronger phase segregation occurred on blending with the PVPh and PAA homopolymers, leading to much more highly ordered mesoporous structures. We have also prepared mesoporous silicas templated by PEO-*b*-PCL/phenolic blends (A-*b*-B/C), where the phenolic acted additionally as a pore expander.[121]

Mesoporous silicas templated by ABC triblock copolymers

Because ABC triblock copolymers can self-assemble into various self-assembled hierarchical structures, these kinds of triblock copolymers can act as the templates to achieve hierarchical mesoporous silicas.[122–125] For example, we have prepared hierarchical mesoporous silicas templated by PE-*b*-PEO-*b*-PCL or PE-*b*-PEO-*b*-PLA triblock copolymer as single templates,[126–128] obtaining mesopores of two different sizes, as confirmed through SAXS, TEM and Brunauer–Emmett–Teller (BET) analyses (Fig. 19).[126,127] The FCC combining tetragonal cylinder structures have been observed using TEM (Figs 19(l)–19(n), from the [001], [10], [11] directions, respectively). Tetragonal packing with two different pore sizes is observed in Fig. 19(l), with smaller mesopores (3.8 nm) formed because of the PE segment and larger cylindrical mesopores (8.6 nm) formed because of the PCL segment, similar to the findings of BET analyses (Fig. 19(k)). An FCC combined with tetragonal cylinder structure, viewed from the [10] direction, is displayed in Fig. 19(m), and a spherical structure observed around the 2_1 helix (zigzag-like) wall, viewed from the [11] direction, is presented in Fig. 19(n). In addition, we prepared PE-*b*-PEO-*b*-PCL with various lengths of PCL blocks and used them as single templates in the preparation of hierarchical mesoporous silicas (Fig. 19(a)). We observed an alternate BCC hierarchical nanostructure templated by the PE_{13}-*b*-PEO_{42}-*b*-PCL_9 triblock copolymer, where the crystallographic sites possessed one BCC structure occupied at (1/4, 1/4, 1/4) and the other occupied at (0, 0, 0), as revealed by TEM (Figs 19(b)–19(d)), the corresponding fast Fourier transform (FFT) patterns (Figs 19(e)–19(g)) and the corresponding phase structures (Figs 19(h)–19(j)) viewed from the [100], [110], [210] planes.[126,127] Furthermore, we have also used PE-*b*-PEO-*b*-PLA as a single template to synthesize a hierarchical mesoporous silica and observed similar tetragonal cylinders with FCC structures.[128] When applying this mesoporous silica for the loading of fluorescein isothiocyanate isomers, we found that the maximum drug loading capacity was 90.4 μg mg^{-1}.

 © 2021 Society of Industrial Chemistry.

10970126, 2022, 4, Downloaded from https://onlinelibrary.wiley.com/doi/10.1002/pi.6264 by National Sun-Yat-Sen, Wiley Online Library on [15/11/2022]. See the Terms and Conditions (https://onlinelibrary.wiley.com/terms-and-conditions) on Wiley Online Library for rules of use; OA articles are governed by the applicable Creative Commons License

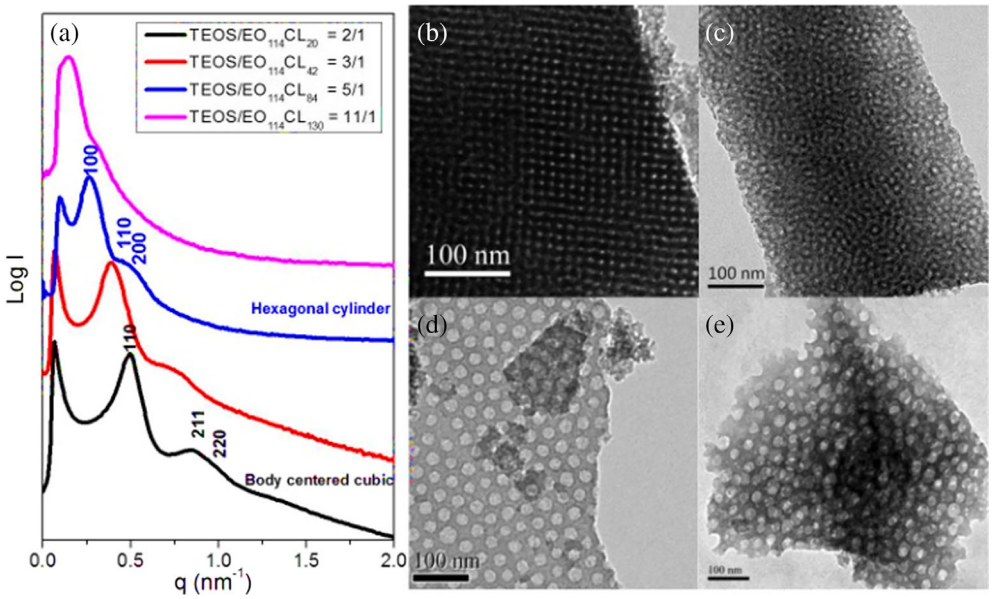

Figure 18. (a) SAXS patterns and (b)–(e) TEM images of mesoporous silicas templated by PEO_{114}-*b*-PCL_n at various weight fractions: (b) TEOS/PEO_{114}-*b*-PCL_{20} = 2/1, (c) TEOS/PEO_{114}-*b*-PCL_{42} = 3/1, (d) TEOS/PEO_{114}-*b*-PCL_{84} = 5/1 and (e) TEOS/PEO_{114}-*b*-PCL_{130} = 11/1.[116]

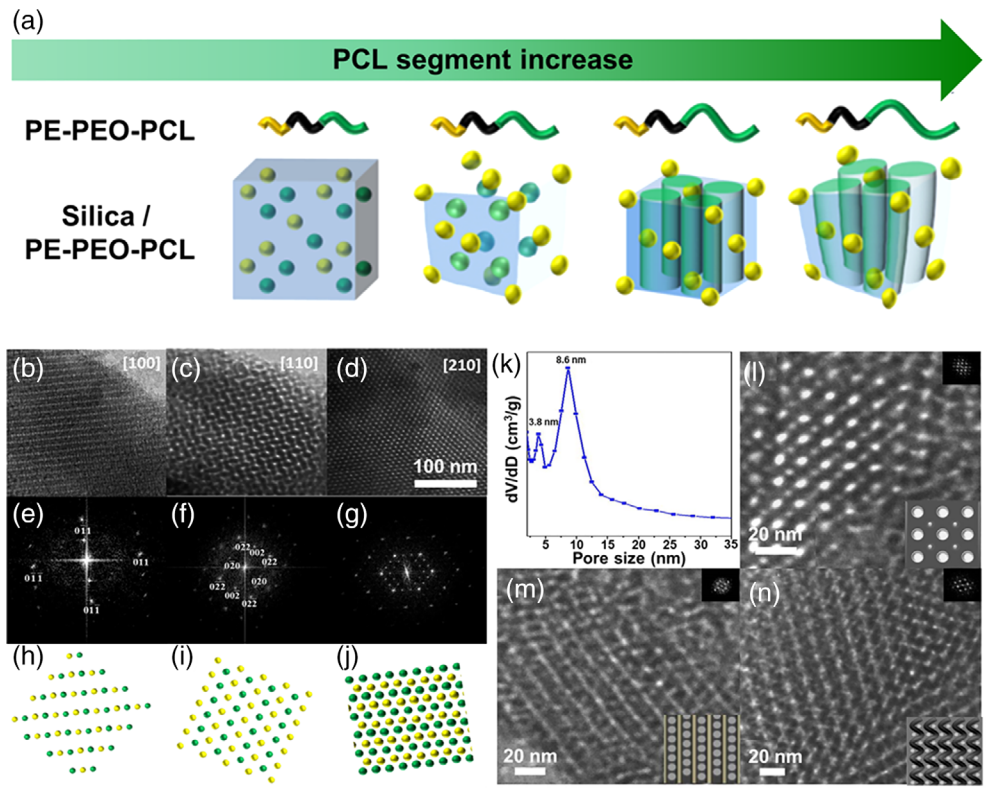

Figure 19. (a) Hierarchical mesoporous silicas templated by PE-*b*-PEO-*b*-PCL triblock copolymers featuring PCL segments of various chain lengths. (b)–(d) TEM images, (e)–(g) FFT patterns and (h)–(j) phase diagrams viewed from the (h) [100], (i) [110] and (j) [210] directions of the alternative BCC structures templated by PE_{13}-*b*-PEO_{42}-*b*-PCL_9. (k) Pore size distribution curve and (l)–(n) TEM images viewed from the (l) [001], (m) [10] and (n) [11] directions (inset: FFT pattern) of the tetragonal cylinders with FCC structures templated by PE_{13}-*b*-PEO_{42}-*b*-PCL_{31}.[126,127]

Mesoporous phenolic/carbon materials

Mesoporous phenolic/carbon materials templated by block copolymers

Much like mesoporous silicas, mesoporous phenolic and carbon materials displaying high pore volumes and surface areas also have many interesting applications in catalysis, adsorption, photonics and separation. In general, there are two types of phenolic resin: novolac and resol. Similar to the preparation of mesoporous silicas, mesoporous phenolic resins are formed in several steps: (i) thermal curing of the phenolic in an acidic

 © 2021 Society of Industrial Chemistry.

10970126, 2022, 4, Downloaded from https://onlinelibrary.wiley.com/doi/10.1002/pi.6264 by National Sun-Yat-Sen, Wiley Online Library on [15/11/2022]. See the Terms and Conditions (https://onlinelibrary.wiley.com/terms-and-conditions) on Wiley Online Library for rules of use; OA articles are governed by the applicable Creative Commons License

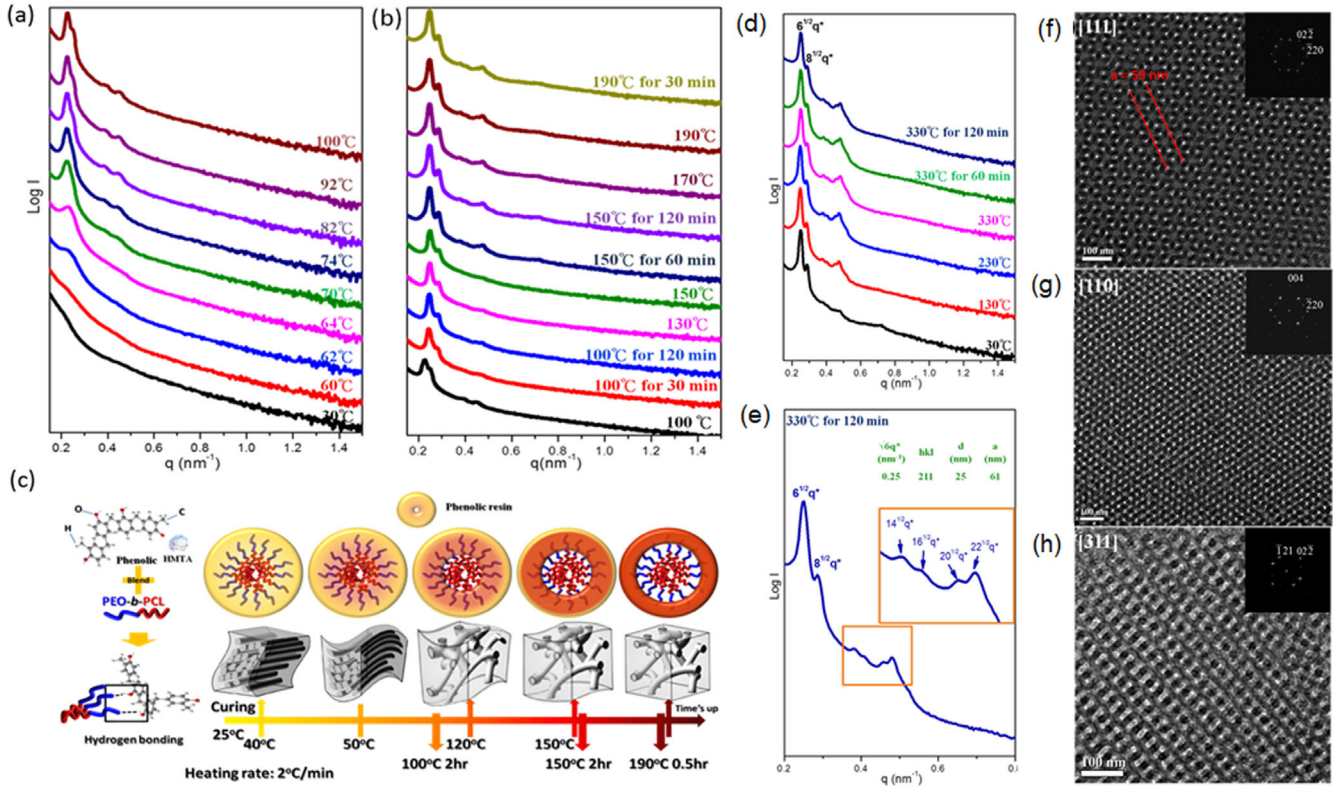

Figure 20. (a), (b) *In situ* SAXS patterns of phenolic/PEO-*b*-PCL/HMTA mixtures recorded during thermal curing and (c) schematic representation of the mesophase transformation. (d) *In situ* SAXS patterns of self-assembled phenolic recorded during thermal calcination. (e) Enlarged SAXS pattern of the mesoporous phenolic after thermal calcination. (f)–(h) TEM images of the mesoporous phenolic with DG structure viewed from the (f) [111], (g) [110] and (h) [311] directions.[141]

or basic medium, (ii) self-assembly in block copolymer/phenolic blends during a thermal curing process, (iii) removal of the template and (iv) carbonization.[129–131] Many long-range-ordered mesoporous phenolic/carbon materials have been prepared using F127, P123, PS-*b*-P4VP, PEO-*b*-PCL, PEO-*b*-PLA, PEO-*b*-PS, PEO-*b*-PMMA and PEO-*b*-poly(γ-benzyl-L-glutamate) (PBLG) as templates.[132–152] For instance, we have proposed the synthesis of mesoporous phenolic resins templated by various PEO-*b*-PCL through thermal crosslinking with hexamethylenetetramine (HMTA).[53] Because the K_A value of phenolic/PEO is larger than that of phenolic/PCL binary pairs, a microphase-separation closed-loop phase diagram formed as a result of the ΔK effect. By varying the volume fraction of PEO-*b*-PCL and content of phenolic, mesoporous phases with HPC and DG structures were obtained. After thermal calcination under an N_2 atmosphere, the DG mesoporous phenolic resins were transformed into mesoporous carbons with a high surface area (*ca* 860 $m^2\ g^{-1}$).

To examine the self-assembly behavior of the DG mesoporous phenolic resin, we used *in situ* SAXS patterns to measure the transformations of phenolic/PEO-*b*-PCL mixtures with HMTA (Figs 20(a)–20(c)).[141] The SAXS patterns revealed a transformation from disordered to HPC and, finally, to DG structures under thermal curing, summarized in Figs 20(a), 20(b), through a process of 'reaction-induced microphase separation'. Figure 20(d) displays *in situ* SAXS patterns measured under the thermal calcination process; the highly ordered peaks in a ratio of √6:√8:√14:√16:√20:√22 became sharper as the electron density contrast increased after removal of the template (Fig. 20(e)), as confirmed by TEM images viewed from the [111], [110], [311] planes (Figs 20(f)–20(h)), suggesting Ia$\bar{3}$*d* symmetry.[141]

Mesoporous phenolic/carbon templated by block copolymer/homopolymer

Because mesoporous silicas could be templated by block copolymer/homopolymer, the same concept was applied to the preparation of mesoporous phenolic/carbon materials. For example, Zhao and colleagues obtained large-pore mesoporous carbons templated by PEO-*b*-PMMA/PMMA and PEO-*b*-PS/PS, where the PMMA and PS homopolymers could act as the pore expanders; disordered porous carbons were observed, however, at higher concentrations of the PS and PMMA homopolymers because of macrophase separation occurring at these compositions.[142,143]

By mediating the hydrophilic PEO volume fraction, we obtained the highly ordered mesoporous phenolic templated by the PEO-*b*-PCL/PEO mixture.[144] Using star-type PEO-POSS in place of the PEO homopolymer resulted in the phase diagram presented in Fig. 21(a). The mesoporous phases transformed from LAM to DG to HPC to BCC structures with increase of the volume fraction of the PEO domain, similar to the typical phase diagram of a diblock copolymer (Fig. 21(b)).[144] Recently, we prepared silica-doped mesoporous carbon materials from N-resol phenolic templated by PEO-*b*-PCL/TEOS mixtures; the mesophases transformed from DG to HPC to LAM structures upon increasing the content of TEOS; after removal of the template, such mesoporous carbon/silica materials displayed potential for application as supercapacitors for energy storage.[146]

© 2021 Society of Industrial Chemistry.

10970126, 2022, 4, Downloaded from https://onlinelibrary.wiley.com/doi/10.1002/pi.6264 by National Sun-Yat-Sen, Wiley Online Library on [15/11/2022]. See the Terms and Conditions (https://onlinelibrary.wiley.com/terms-and-conditions) on Wiley Online Library for rules of use; OA articles are governed by the applicable Creative Commons License

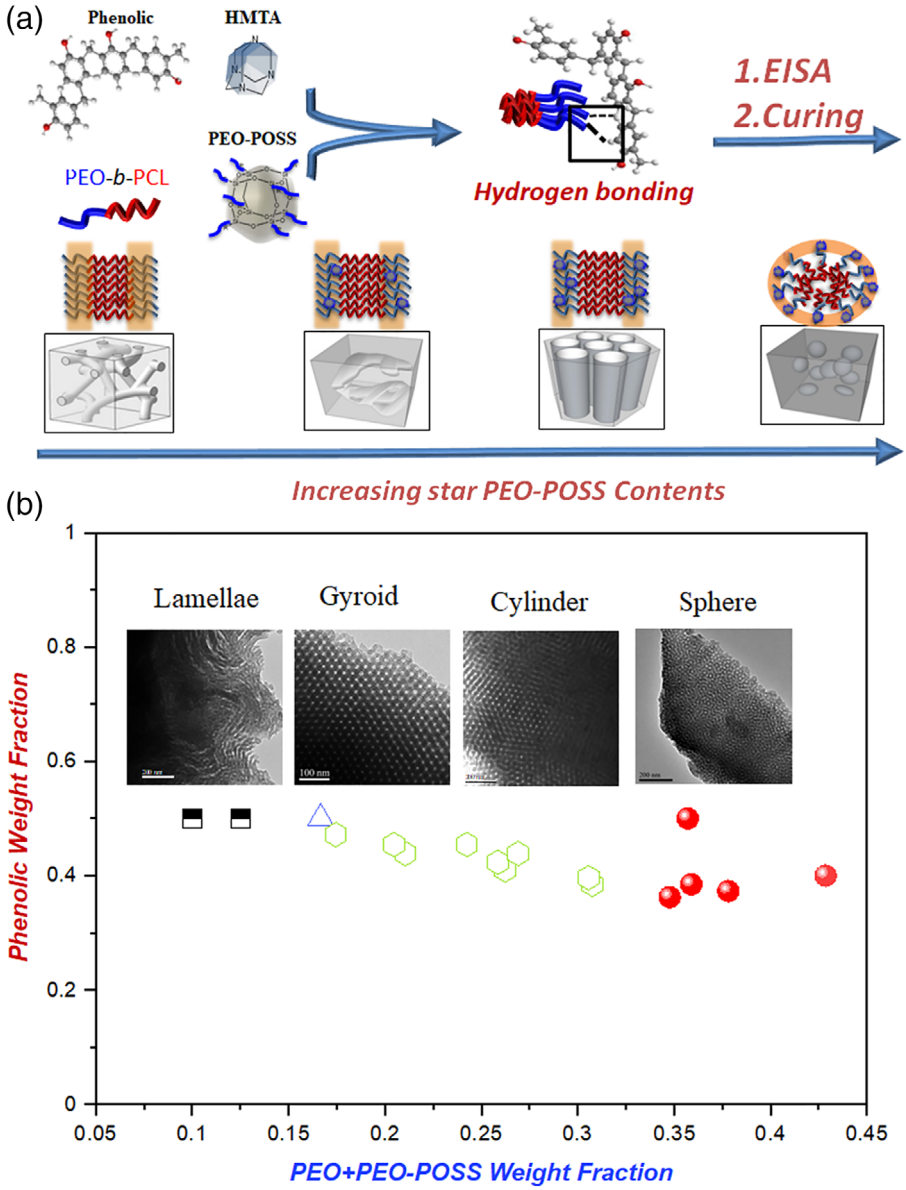

Figure 21. (a) Mesoporous phenolic structures templated by PEO-*b*-PLC/PEO-POSS blends at various PEO-POSS concentrations, with HMTA as the curing agent. (b) Phase diagram of mesoporous phenolic structures templated by PEO-*b*-PLC/PEO-POSS blends containing various weight fractions of PEO + PEO-POSS.[144]

Mesoporous phenolic/carbon materials templated by ABC triblock copolymers

ABC copolymers can be used as the single templates to synthesize mesoporous phenolic/carbon. For example, mesoporous carbons have been obtained from resol/PEO-*b*-PMMA-*b*-PS and resol/PEO-*b*-PS-*b*-PI blends.[153,154] Because the hydrogen bonding in phenolic/PEO blends is stronger than in phenolic/PMMA blends, the pore wall thickness could be varied by changing the ratio of the blocks in the triblock copolymer. In addition, carbon materials with highly ordered and large mesopores (*ca* 39 nm) have been obtained using PEO-*b*-PS-*b*-PI as the template.[148] We have prepared a mesoporous phenolic templated by PEO-*b*-PCL-*b*-(poly-L-lactic acid) (PLLA) with HMTA (Fig. 22(a)).[155] These phenolic/PEO-*b*-PCL-*b*-PLLA blends possessed the following gradient in their hydrogen bonding strengths: phenolic/PEO > phenolic/PCL > phenolic/PLLA. Mesoporous phenolic resins featuring disordered, DG, HPC and BCC structures were obtained by varying the content of the phenolic resin (Figs 22(b)–22(e)). At a higher content of phenolic resin (>60 wt%), all of the OH units of the phenolic could interact with the PEO, PCL and PLLA segments, thereby inducing a miscible disordered structure; in contrast, using only 30–50 wt% of the phenolic led to the formation of highly ordered mesoporous structures as a result of greater balance between the phenolic composition and the hydrogen bonding interactions.[155] The use of ABC triblock copolymer as a single template to synthesize hierarchical mesoporous phenolic/carbon structures has not been reported to date since the strongest hydrogen bond units should be located in the B segment while the A/C segments must be immiscible. Such structures remain a future challenge for the design of hierarchical mesoporous phenolic/carbon.

© 2021 Society of Industrial Chemistry.

10970126, 2022, 4, Downloaded from https://onlinelibrary.wiley.com/doi/10.1002/pi.6264 by National Sun-Yat-Sen, Wiley Online Library on [15/11/2022]. See the Terms and Conditions (https://onlinelibrary.wiley.com/terms-and-conditions) on Wiley Online Library for rules of use; OA articles are governed by the applicable Creative Commons License

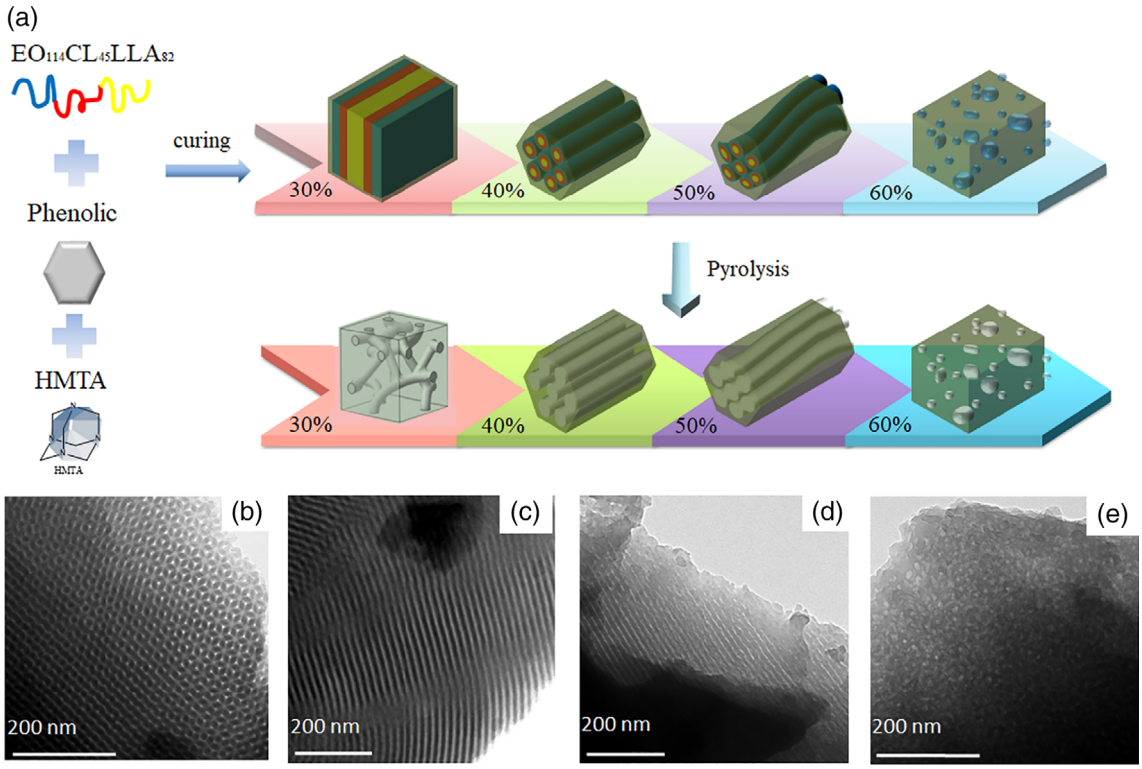

Figure 22. (a) Mesoporous phenolic structures templated by the triblock copolymer PEO_{114}-*b*-PCL_{45}-*b*-$PLLA_{82}$ with HMTA as the curing agent. (b)–(e) Corresponding TEM images of mesoporous phenolic structures templated by phenolic/PEO_{114}-*b*-PCL_{45}-*b*-$PLLA_{82}$ with (b) 30/70, (c) 40/60, (d) 50/50 and (e) 60/40.[155]

CONCLUSIONS

This review summarizes the recent progress made in the use of hydrogen bonding to mediate the formation of self-assembled structures from block copolymer/homopolymer and block copolymer mixtures in the bulk state. By varying the copolymer composition and the volume fractions of blocks in the copolymer mixtures, various self-assembled structures can be obtained, including typical LAM, DG, HPC and BCC structures as well as such hierarchical structures as three-phase LAM, core/shell HPC, HPC in LAM, core/shell DG, and even Archimedean tiling patterns. Using this concept of hydrogen-bond-mediated self-assembly of block copolymer mixtures, it is also possible to synthesize mesoporous silica, phenolic and carbon materials. The construction of these hierarchically mesoporous materials is interesting to both academia and industry, with various diverse potential applications in, for example, photocatalysis, CO_2 uptake, energy storage and conversion, and drug delivery. A challenge remains, however, to develop approaches for the design of hierarchical mesoporous materials with new Archimedean tiling patterns and Frank–Kasper phases.[156,157]

ACKNOWLEDGEMENTS

This study was supported financially by the Ministry of Science and Technology, Taiwan, under contracts MOST 108-2638-E-002-003-MY2.

REFERENCES

1 Kim JK, Yang SY, Lee YM and Kim Y, *Prog Polym Sci* **35**:1325–1349 (2010).
2 Ji SY, Zhang RR, Zhang LS, Yuan Y and Lin JP, *Polym Int* **69**:728–736 (2020).
3 Glier TE, Vakili M and Trebbin M, *J Polym Res* **27**:333 (2020).
4 Yuan QQ, Russell TP and Wang D, *Macromolecules* **53**:10981–10987 (2020).
5 Raybin J, Ren J, Chen X, Gronheid R, Nealey P and Sibener SJ, *Nano Lett* **17**:7717–7723 (2017).
6 Albert JNL and Epps TH III, *Mater Today* **13**:24–33 (2010).
7 Zhu GJ, Cheng SW, Hu Y, Li W and Mu JS, *J Polym Res* **27**:124 (2020).
8 Lin EL, Hsu WL and Chiang YW, *ACS Nano* **12**:485–493 (2018).
9 Klok HA and Lecommandoux S, *Adv Mater* **13**:1217–1229 (2001).
10 Yu YG, Seo C, Chae CG, Seo HB, Kim MJ, Kang Y *et al.*, *Macromolecules* **52**:4349–4358 (2019).
11 Hernandez JR, FCY G and Lecommandoux S, *Prog Polym Sci* **30**:691–724 (2005).
12 Matsen MW and Schick M, *Curr Opin Colloid Interface Sci* **1**:329–326 (1996).
13 Lin RC and Kuo SW, *Acta Polym Sin* **8**:789–805 (2018).
14 Li PC, Lin YC, Chen M and Kuo SW, *Soft Matter* **9**:11257–11269 (2013).
15 Kuo SW, *Hydrogen Bonding in Polymeric Materials*. Wiley-VCH, Weinheim (2018).
16 Zhang L and Eisenberg A, *J Am Chem Soc* **118**:3168–3181 (1996).
17 Mai Y and Eisenberg A, *Chem Soc Rev* **41**:5969–5985 (2012).
18 Peng H, Chen D and Jiang M, *Langmuir* **19**:10989–10992 (2003).
19 Zhu J, Yu H and Jiang W, *Macromolecules* **38**:7492–7501 (2005).
20 Ruokolainen J, ten-Brinke G and Ikkala O, *Macromolecules* **29**:3409–3415 (1996).
21 Ruokolainen J, Torkkeli M, Serimaa R, Komanschek E, ten-Brinke G and Ikkala O, *Macromolecules* **30**:2002–2007 (1997).
22 Ruokolainen J, Tanner J, Ikkala O, ten-Brinke G and Thomas EL, *Macromolecules* **31**:3532–3353 (1998).
23 Ruokolainen J, Makinen R, Torkkeli M, Makela T, Serimaa R, ten-Brinke G *et al.*, *Science* **280**:557–560 (1998).
24 Chen SC, Kuo SW and Chang FC, *Langmuir* **27**:10197–10205 (2011).
25 Tanaka H, Hasegawa H and Hashimoto T, *Macromolecules* **24**:240–251 (1991).
26 Kuo SW, *Polym Int* **58**:455–464 (2009).

© 2021 Society of Industrial Chemistry.

10970126, 2022, 4, Downloaded from https://onlinelibrary.wiley.com/doi/10.1002/pi.6264 by National Sun-Yat-Sen, Wiley Online Library on [15/11/2022]. See the Terms and Conditions (https://onlinelibrary.wiley.com/terms-and-conditions) on Wiley Online Library for rules of use; OA articles are governed by the applicable Creative Commons License

27 Zhao JQ, Pearce EM and Kwei TK, *Macromolecules* **30**:7119–7126 (1997).
28 Kuo SW, *J Polym Res* **15**:459–486 (2008).
29 Kosoneen H, Ruokolainen J, Nyholm P and Ikkala O, *Polymer* **42**:9481–9486 (2001).
30 Dobrosielska K, Wakao S, Takano A and Matsushita Y, *Macromolecules* **41**:7695–7698 (2008).
31 Dobrosielska K, Wakao S, Suzuki J, Noda K, Takano A and Matsushita Y, *Macromolecules* **42**:7098–7102 (2009).
32 Chen SC, Kuo SW, Jeng US, Su CJ and Chang FC, *Macromolecules* **43**:1083–1092 (2010).
33 Tsai SC, Lin YC, Lin EL, Chiang YW and Kuo SW, *Polym Chem* **7**:2395–2409 (2016).
34 Dehghan A and Shi AC, *Macromolecules* **46**:5796–5805 (2013).
35 Jang SG, Kramer EJ and Hawker CJ, *J Am Chem Soc* **133**:16986–16996 (2011).
36 Gai Y, Lin Y, Song DP, Yavitt BM and Watkins JJ, *Macromolecules* **49**:3352–3360 (2016).
37 Li JH, Li Y, Xu JT and Luscombe CK, *ACS Appl Mater Interfaces* **9**:17942–17948 (2017).
38 Yeh SW, Chang YT, Chou CH and Wei KH, *Macromol Rapid Commun* **25**:1679–1686 (2004).
39 Noro A, Asai H, Higuchi K and Matsushita Y, *ACS Appl Polym Mater* **1**:3432–3442 (2019).
40 Wu YR, Wu YC and Kuo SW, *Macromol Chem Phys* **214**:1496–1503 (2013).
41 Lu YS and Kuo SW, *RSC Adv* **4**:34849–34859 (2014).
42 Lu YS, Yu CY, Lin YC and Kuo SW, *Soft Matter* **12**:2288–2300 (2016).
43 Lu YS, Baskakoti BP, Pramanik M, MSA H, Alshehri SM, Yamauchi Y *et al.*, *RSC Adv* **6**:106866–106872 (2016).
44 Chiou CW, Lin YC, Wang L, Maeda R, Hayakawa T and Kuo SW, *Macromolecules* **47**:8709–8721 (2014).
45 Yu CY and Kuo SW, *Ind Eng Chem Res* **57**:2546–2559 (2018).
46 Su WC, Wu YS, Wang CF and Kuo SW, *Crystals* **8**:330 (2018).
47 Hameed N and Guo Q, *Polymer* **49**:5268–5275 (2008).
48 Hameed N, Liu J and Guo Q, *Macromolecules* **41**:7596–7605 (2008).
49 Hameed N and Guo Q, *Polymer* **49**:922–933 (2008).
50 Chen WC, Kuo SW, Lu CH, Jeng US and Chang FC, *Macromolecules* **42**:3580–3590 (2009).
51 Balsamo V, von Gyldenfeldt F and Stadler R, *Macromolecules* **32**:1226–1232 (1999).
52 Salim NV, Hanley T and Guo Q, *Macromolecules* **43**:7695–7704 (2010).
53 Li JG, Lin YD and Kuo SW, *Macromolecules* **44**:9295–9309 (2011).
54 Salim NV, Hameed N and Guo Q, *J Polym Sci B* **47**:1894–1905 (2009).
55 Lu CH, Kuo SW, Chang WT and Chang FC, *Macromol Rapid Commun* **30**:2121–2127 (2009).
56 Hameed N, Salim NV and Guo Q, *J Chem Phys* **131**:214905 (2009).
57 Su WC, Tsai FC, Huang CF, Dai L and Kuo SW, *Polymers* **11**:201 (2019).
58 Chu WC, Li JG, Wang CF, Jeong KW and Kuo SW, *J Polym Res* **20**:1–9 (2013).
59 Chu WC, Li JG and Kuo SW, *RSC Adv* **3**:6485–6498 (2013).
60 Menestrel CL, Bhagwagar DE, Painter PC, Coleman MM and Graf JF, *Macromolecules* **25**:7101–7106 (1992).
61 Hong BK, Kim JY and Jo WH, *Polymer* **38**:4373–4735 (1997).
62 Kuo SW, Lin CL and Chang FC, *Macromolecules* **35**:278–285 (2002).
63 Coleman MM and Painter PC, *Prog Polym Sci* **20**:1–59 (1995).
64 Lee HF, Kuo SW, Huang CF, Lu JS, Chan SC, Wang CF *et al.*, *Macromolecules* **39**:5458–5465 (2006).
65 Chen WC, Kuo SW, Jeng U and Chang FC, *Macromolecules* **41**:1401–1410 (2008).
66 Zhou J and Shi AC, *J Chem Phys* **130**:234904 (2009).
67 Lin I, Kuo SW and Chang FC, *Polymer* **50**:5276–5287 (2009).
68 Han SH, Pryamitsyn V, Bae D, Kwak J, Ganesan V and Kim JK, *ACS Nano* **6**:7966–7972 (2012).
69 Kwak J, Han SH, Moon HC, Kim JK, Koo J, Lee JS *et al.*, *Macromolecules* **48**:1262–1266 (2015).
70 Pryamitsyn V, Han SH, Kim JK and Ganesan V, *Macromolecules* **45**:8729–8742 (2012).
71 Han SH and Kim JK, *Macromolecules* **44**:4970–4976 (2011).
72 Kwak J, Han SH, Moon HC and Kim JK, *Macromolecules* **48**:6347–6352 (2015).
73 Gido SP, Schwark DW, Thomas EL and Goncalves M, *Macromolecules* **26**:2636–2640 (1993).
74 Rzayev J and Hillmyer MA, *Macromolecules* **38**:3–5 (2005).
75 Daubian D, Fillion A, Gaitzsch J and Meier W, *Macromolecules* **53**:11040–11050 (2020).
76 Dong S and Li W, *Macromolecules* **54**:203–213 (2021).
77 Xie Q, Qiang Y and Li W, *ACS Macro Lett* **9**:278–283 (2020).
78 Huang CF, Chen WH, Aimi J, Huang YS, Venkatesan S, Chiang YW *et al.*, *Polym Chem* **9**:5644–5654 (2018).
79 Tsai CC, Gan Z, Chen T and Kuo SW, *Macromolecules* **51**:3017–3029 (2018).
80 Chiang YW, Hu YY, Li JN, Huang SH and Kuo SW, *Macromolecules* **48**:8526–8533 (2015).
81 Matsushita Y, *Macromolecules* **40**:771–776 (2007).
82 Tsou CT and Kuo SW, *Macromolecules* **52**:8374–8383 (2019).
83 Asari T, Matsuo S, Takano A and Matsushita Y, *Macromolecules* **38**:8811–8815 (2005).
84 Chen WC, Kuo SW and Chang FC, *Polymer* **51**:4176–4184 (2010).
85 Tseng TC and Kuo SW, *Macromolecules* **51**:6451–6459 (2018).
86 Tseng TC and Kuo SW, *Molecules* **23**:2242 (2018).
87 Tseng TC and Kuo SW, *Eur Polym J* **116**:361–369 (2019).
88 Jiang S, Gopfert A and Abetz V, *Macromolecules* **36**:6171–6177 (2003).
89 Asari T, Arai S, Takano A and Matsushita Y, *Macromolecules* **39**:2232–2237 (2006).
90 Miyase H, Asai Y, Takano A and Matsushita Y, *Macromolecules* **50**:979–986 (2017).
91 Zhang W, Shi L, Gao L, An Y, Li G, Wu K *et al.*, *Macromolecules* **38**:899–903 (2005).
92 Gao WP, Bai Y, Chen EQ, Li ZC, Han BY, Yang WT *et al.*, *Macromolecules* **39**:4894–4898 (2006).
93 Lee SC, Kim KJ, Jeong YK, Chang JH and Choi J, *Macromolecules* **38**:9291–9297 (2005).
94 Matejicek P, Uchman M, Lokajova J, Stepanek M, Prochazka K and Spirkova M, *J Phys Chem B* **111**:8394–8401 (2007).
95 Lefevre N, Fustin CA and Gohy JF, *Macromol Rapid Commun* **30**:1871–1888 (2009).
96 Talingting MR, Munk P, Webber SE and Tuzar Z, *Macromolecules* **32**:1593–1601 (1999).
97 Li G, Shi L, Ma R, An Y and Haung N, *Angew Chem Int Ed* **118**:5081–5084 (2006).
98 Xiong D, He Z, An Y, Li Z, Wang H, Chen X *et al.*, *Polymer* **49**:2548–2522 (2008).
99 Xiong D, Shi L, Jiang X, An Y, Chen X and Lu J, *Macromol Rapid Commun* **28**:194–199 (2007).
100 Gao Y, Wei Y, Li B and Han Y, *Polymer* **49**:2354–2361 (2008).
101 Huang W, Luo C, Li B and Han Y, *Macromolecules* **39**:8075–8082 (2006).
102 Xie D, Xu K, Bai R and Zhang G, *J Phys Chem B* **111**:778–781 (2007).
103 Kuo SW, Tung PH, Lai CL, Jeong KU and Chang FC, *Macromol Rapid Commun* **29**:229–233 (2008).
104 Kuo SW, Tung PH and Chang FC, *Eur Polym J* **45**:1924–1935 (2009).
105 Hsu CH, Kuo SW, Chen JK, Ko FH, Liao CS and Chang FC, *Langmuir* **24**:7727–7734 (2008).
106 Zhao D, Feng J, Huo Q, Melosh N, Fredrickson GH, Chmelka BF *et al.*, *Science* **279**:548–552 (1998).
107 Wan Y and Zhao D, *Chem Rev* **107**:2821–2860 (2007).
108 Brinker J, Lu Y, Sellinger A and Fan H, *Adv Mater* **11**:579–585 (1999).
109 Soler-Illia GJ, Crepaldi EL, Grosso D and Sanchez C, *Curr Opin Colloid Interface Sci* **8**:109–126 (2003).
110 Chu WC, Chiang SF, Li JG and Kuo SW, *RSC Adv* **4**:784–793 (2014).
111 Deng Y, Yu T, Wang Y, Shi Y, Meng Y, Gu D *et al.*, *J Am Chem Soc* **29**:1690–1697 (2007).
112 Bloch E, Llewellyn PL, Phan T, Bertin D and Hornebecq V, *Chem Mater* **21**:48–55 (2009).
113 Wei J, Wang H, Deng Y, Sun Z, Shi L, Tu B *et al.*, *J Am Chem Soc* **133**:20369–20377 (2011).
114 Li JG, Chen WC and Kuo SW, *Microporous Mesoporous Mater* **163**:34–41 (2012).
115 Li JG and Kuo SW, *RSC Adv* **1**:1822–1833 (2011).
116 Li JG, Chang YH, Lin YS and Kuo SW, *RSC Adv* **2**:12973–12982 (2012).
117 Chu WC, Lin CX and Kuo SW, *RSC Adv* **4**:61012–61021 (2014).
118 Altukhov O and Kuo SW, *RSC Adv* **5**:22625–22637 (2015).
119 Li JG, Chu WC, Tu CW and Kuo SW, *J Nanosci Nanotechnol* **13**:2495–2506 (2013).
120 Tirumala VR, Pai RA, Agarwal S, Testa JJ, Bhatnagar G, Romang AH *et al.*, *Chem Mater* **19**:5868–5874 (2007).
121 Chu WC, Dai L, Chen JK, Huang CF and Kuo SW, *J Nanosci Nanotechnol* **16**:9805–9092 (2016).

© 2021 Society of Industrial Chemistry.

10970126, 2022, 4, Downloaded from https://onlinelibrary.wiley.com/doi/10.1002/pi.6264 by National Sun-Yat-Sen, Wiley Online Library on [15/11/2022]. See the Terms and Conditions (https://onlinelibrary.wiley.com/terms-and-conditions) on Wiley Online Library for rules of use; OA articles are governed by the applicable Creative Commons License

122 Innocenzi P, Malfatti L and GJAA S-III, *Chem Mater* **23**:2501–2509 (2011).
123 Wei J, Yue Q, Sun Z, Deng Y and Zhao D, *Angew Chem Int Ed* **124**: 6253–6257 (2012).
124 Liu CC, Li JG and Kuo SW, *RSC Adv* **4**:20262–20272 (2014).
125 Chu WC, Peng DR, Bastakoti BP, Pramanik M, Malgras V, Ahamad T *et al*., *ChemistrySelect* **1**:1339–1346 (2016).
126 Li JG, Lin RB and Kuo SW, *Macromol Rapid Commun* **33**:678–682 (2012).
127 Li JG, Lin RB and Kuo SW, *RSC Adv* **3**:17411–17423 (2013).
128 Chu WC, Cheng CC, Bastakoti BP and Kuo SW, *RSC Adv* **6**:33811–33820 (2016).
129 Langley PJ and Hulliger J, *Chem Soc Rev* **28**:279–291 (1999).
130 Dawson R, Cooper AI and Adams DJ, *Prog Polym Sci* **37**:530–563 (2012).
131 Muylaert I, Verberckmoes A, Decker JD and Voort PVD, *Adv Colloid Interface Sci* **175**:39–51 (2012).
132 Kosonen H, Ruokolainen J, Torkkeli M, Serimaa R, Nyholm P and Ikkala O, *Macromol Chem Phys* **203**:388–392 (2002).
133 Liang C and Dai S, *J Am Chem Soc* **128**:5316–5317 (2006).
134 Meng Y, Gu D, Zhang F, Shi Y, Cheng L, Feng D *et al*., *Chem Mater* **18**: 4447–4464 (2006).
135 Chu WC, Chiang SF, Li JG and Kuo SW, *Materials* **6**:5077–5093 (2013).
136 Valkama S, Nykanen A, Kosonen H, Ramani R, Tuomisto F, Engelhardt P *et al*., *Adv Funct Mater* **17**:183–190 (2007).
137 Kosenen H, Valkama S, Nykanen A, Toivanen M, ten-Brinke G, Ruokolainen J *et al*., *Adv Mater* **18**:201–205 (2006).
138 Liang C, Hong K, Guiocheon GA, Mays JW and Dai S, *Angew Chem Int Ed* **43**:5785–5789 (2004).
139 Hu D, Xu Z, Zeng K and Zheng S, *Macromolecules* **43**:2960–2969 (2010).
140 Deng Y, Liu C, Gu D, Yu T, Tu B and Zhao D, *J Mater Chem* **18**:91–97 (2008).
141 Li JG, Chu WC, Jeng U and Kuo SW, *Macromol Chem Phys* **51**:2115–2123 (2013).
142 Deng Y, Liu J, Liu C, Gu D, Sun Z, Wei J *et al*., *Chem Mater* **20**:7281–7286 (2008).
143 Wei J, Deng Y, Zhang J, Sun Z, Tu B and Zhao D, *Solid State Sci* **13**:84–792 (2011).
144 Li JG, Chung CY and Kuo SW, *J Mater Chem* **22**:18583–18595 (2012).
145 AFM EL-M, Yu TC, Mohamed MG and Kuo SW, *Macromolecules* **54**: 1030–1042 (2021).
146 AFM EL-M, Yu TC and Kuo SW, *Chem Eng J* **414**:128796 (2021).
147 AFM EL-M, Liu TE and Kuo SW, *J Hazard Mater* **391**:122163 (2020).
148 Mohamed MG, Hung WS, AFM EL-M, MMM A, Dai L, Chen T *et al*., *Polymers* **12**:1193 (2020).
149 Hung WS, Ahmed MMM, Mohamed MG and Kuo SW, *J Polym Res* **27**: 173 (2020).
150 Li JG, Lee PY, Ahmed MMM, Mohamed MG and Kuo SW, *Macromol Chem Phys* **221**:2000040 (2020).
151 Li JG, Ho YF, Ahmed MMM, Liang HC and Kuo SW, *Chem A Eur J* **25**: 10456–10463 (2019).
152 Chu WC, Bastakoti BP, Kaneti YV, Li JG, Alamri HR, Alothman ZA *et al*., *Chem A Eur J* **35**:13734–13741 (2017).
153 Zhang J, Deng Y, Wei J, Sun Z, Gu D, Bongard H *et al*., *Chem Mater* **21**: 3996–4005 (2009).
154 Werner JG, Hoheisel TN and Wiesner U, *ACS Nano* **8**:731–743 (2014).
155 Liu CC, Chu WC, Li JG and Kuo SW, *Macromolecules* **47**:6389–6400 (2014).
156 Mohamed MG, Atayde E Jr, Matsagar BM, Na J, Yamauchi Y, KCW W *et al*., *J Taiwan Inst Chem Eng* **112**:180–192 (2020).
157 Abuzeid HR, AFM EL-M and Kuo SW, *Giant* **6**:100054 (2021).

© 2021 Society of Industrial Chemistry.

10970126, 2022, 4, Downloaded from https://onlinelibrary.wiley.com/doi/10.1002/pi.6264 by National Sun-Y at-Sen, Wiley Online Library on [15/11/2022]. See the Terms and Conditions (https://onlinelibrary.wiley.com/terms-and-conditions) on Wiley Online Library for rules of use; OA articles are governed by the applicable Creative Commons License